Chapter three:

Methodology

3.1. Introduction:

The research idea in the investigation of using the CSP technology in generating the steam required for steam flooding is basically can be summarized in three element the first part discuss the compatibly of the location to CSP requirement which is presented in term of direct normal radiation (DNI) and land usage second is studying the effect of the limitation of CSP technology on the reservoir, the limited supply of steam in just day time made the full solar steam injections limited during day time and can be extend for few hours by thermal storage backup so for the project to be completely independent of fossil fuel the injection rate must not be continues and constant, the effect of not continues rate injection can be studied with application of reservoir simulation , the third element is the economic and financial

Section one:

Solar Radiation and Meteorology Data:

Solar Potential at Fula North East (FNE) field location will be studied base on Direct Normal Irradiation (DNI), since it represent the meteorological parameter that has the strongest influence on performance of a CSP plant.[Kaushal Chhatbar]

3.2.1. Comparisons Solar Radiation and Meteorological parameters between FNE and Amal oilfields location:

The investigating of FNE oilfield compatibility to Concentrating Solar Power (CSP) applications was based on comparing solar radiation and meteorological data in field location with existing solar thermal EOR project at Amal field in Southern Oman.

Amal oil field in Oman was selected to be a benchmarked for his study not only because the availability of the project data, but also because the one year pilot project conducted in the field has demonstrated the technical feasibility of solar steam generation for EOR in the field location and desert condition, also the actual performance has match the modeled performance to within a few percent, and the steam output continues to exceed the contract target performance in all tests, while the uptime of the solar field reach 98.6% and continues to improve to be over 99% [Daniel Plamer et al, 2013].

Solar energy and meteorology data for FNE field location was obtained from Surface meteorology and Solar Energy (SSE) - NASA public Data and commercial Meteonorm7 software at field location coordinates (latitude and longitude), database and accuracy for both SSE and Meteonorm7 are included in this chapter.

As for Amal field Direct Normal Irradiation (DNI) data were obtained from Daniel Plamer (et al) paper which discuss the construction, operation, ad performance of the first ecloth through solar steam generation pilot for EOR application. Where the solar data was analyzed and a "Model Year" was present as an average year in term of total radiation, and contains typical weather related variation and was selected as a reference [Daniel Plamer et al, 2013]. In addition the data obtained from Surface

meteorology and Solar Energy (NASA) and Meteonorm7 software based on the field location coordinates.

The comparison made using surface (SSE) and meteonorm7 software between FNE and Amal field locations includes the following solar radiation and meteorological parameters:

- Monthly Average Direct Normal Irradiation (DNI)
- Monthly Averaged Air Temperature.
- Monthly Averaged Wind Speed.
- Monthly Averaged Relative Humidity.
- Precipitation

3.2.1.1. Surface Meteorology and Solar Energy (SSE) –NASA- Release 6.0:

NASA, through its' Science Mission Directorate, has long supported satellite systems and research providing data important to the study of climate and climate processes. These data include long-term estimates of meteorological quantities and surface solar energy fluxes. These satellite and modeled based products have been shown to be accurate enough to provide reliable solar and meteorological resource data over regions where surface measurements are sparse or nonexistent, and offer two unique features - the data is global and, in general, contiguous in time. These two important characteristics, however, tend to generate very large data archives which can be intimidating for commercial users, particularly new users with little experience or resources to explore these large data sets. Moreover the data products contained in the various NASA archives are often in formats that present challenges to new users.

To foster the commercial use of the global solar and meteorological data, NASA supported, and continues to support, the development of the Surface meteorology and Solar Energy (SSE) dataset that has been formulated specifically for photovoltaic and renewable energy system design needs. Of equal importance is the access to these data; to this end the SSE parameters are available via user-friendly web-based applications founded on user needs.

3.2.1.1.1. SSE Release 6.0 Database:

In general, meteorology and solar radiation for SSE Release 6.0 were obtained from the NASA Science Mission Directorate's satellite and re-analysis research programs. Parameters based upon the solar and/or meteorology data were derived and validated based on recommendations from partners in the energy industry. Release 6.0 extends the temporal coverage of the solar and meteorological data from 10 years to more than 22 years (e.g. July 1983 through June 2005) with improved NASA data, and includes new parameters and validation studies

3.2.1.1.2. Surface meteorology and solar energy accuracy :

This section provides estimates of the levels of uncertainty for insulation (solar radiation), temperature, surface pressure, relative humidity, and wind speed through comparisons with ground measurement data. It is generally considered that quality measured data are more accurate than satellite-derived values.

However, measurement uncertainties from calibration drift, operational uncertainties, or data gaps are unknown for ground site data sets. In 1989, the World Climate Research Program estimated that most routine-operation ground sites had "end-to-end" uncertainties from 6 to 12%. Specialized high quality research sites are hopefully more accurate by a factor of two.

Radiation parameters were compared with data from the Baseline Surface Radiation Network (BSRN) (Table 1). Meteorological parameters were compared with data from the National Climate Data Center (NCDC) (Table 2). Wind speeds have been carried over from SSE Release 4 because newer data sets do not provide enough information about vegetation/surface types. The RETScreen Weather Database was used to test uncertainties in the SSE Release 4 wind speeds (Table 3) [Surface meteorology and Solar Energy web site].

Table (3.1): Regression analysis of SSE versus BSRN monthly averaged values for the time period July 1983 through June 2006

Parameter	Region	Bias (%)	RMS (%)
Direct Normal Radiation	Global	-4.06	22.73
	60° Poleward	-15.66	33.12
	60° Equatorward	2.40	20.93

Table (3.2): Linear least squares regression analysis of SSE versus NCDC monthly averaged values for the time period 1983 through 2006

Parameter	Slope	Intercept	R^2	RMSE	Bias
Tmax (°C)	0.99	-1.58	0.95	3.12	-1.83
Tmin (°C)	1.02	0.10	0.95	2.46	0.24
Tavg (°C)	1.02	-0.78	0.96	2.13	-0.58
Tdew (°C)	0.96	-0.80	0.95	2.46	-1.07
RH (%)	0.79	12.72	0.56	9.40	-1.92
Heating Degree Days (degree days)	1.02	12.47	0.93	77.20	17.28
Cooling Degree Days (degree days)	0.86	2.36	0.92	28.90	-5.65
Atmospheric Pressure (hPa)	0.89	102.16	0.74	27.33	-10.20

Table (3.3): Estimated uncertainty for monthly averaged wind speed for the time period July 1983 through June 1993

Parameter	Method	Bias	RMS
Wind Speed at 10 meters for terrain similar to airports (m/s)	A. RET Screen Weather Database (documented 10-m height airport sites)	-0.2	1.3
	B. RET Screen Weather Database (unknown-height airport sites)	-0.0	1.3

3.2.1.2. Meteonorm7 Software:

Meteonorm is a meteorological database containing climatological data for solar engineering applications at every location on the globe. The results are stochastically generated typical years from interpolated long term monthly means. They represent an average year of the selected climatological time period based on the user's settings. As such the results do not rep-resent a real historic year but a hypothetical year which statistically represents a typical year at the selected location.

Meteonorm is primarily a method for the calculation of solar radiation on arbitrarily orientated surfaces at any desired location. The method is based on databases and algorithms coupled according to a predetermined scheme. It commences with the user specifying a particular location for which meteorological data are required, and terminates with the delivery of data of the desired structure and in the required format.

In term of Direct Normal Irradiation Meteonorm depend on Beam radiation, which represent (as describe in the Meteonorm software) is the **direct normal irradiation** (DNI). Shortwave radiation ($\lambda < 3$ μm) arising from a narrow solid angle (5° aperture) centered around the sun's disk and impinging on a surface normal to the

3.2.1.2.1. Software details:

The software basically works in two steps. In a first step, surrounding weather stations are searched and their long-term monthly means are interpolated to the specified location. Data derived from satellite imagery help to improve radiation parameters in regions with a low density of available ground-based data

Figure (3.1): First Step

In a second step, a stochastic weather generator runs on the interpolated monthly data to generate a typical mean year of data in hourly resolution (8'760 values per parameter) for most of the output for-mats. Some of the output formats even require minute-by-minute time resolution

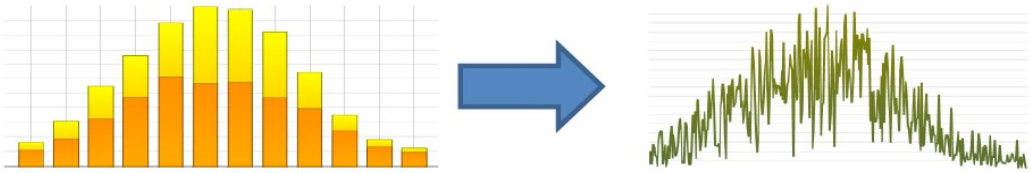

Figure(3.2): step two

3.2.1.2.2. Meteoorm7 Database (Climatological Data):

(A) Ground stations:

In Meteonorm, several databases have been thoroughly checked to ensure reliability and were coupled to form a single comprehensive database permitting worldwide simulation of solar energy systems, buildings and environmental simulations. The database contains all necessary parameters for further processing (global radiation, temperature, wind, humidity and precipitation).

For worldwide applications, several different international databases are included. Global radiation data was taken from the GEBA Global Energy Balance Archive (WMO World Climate Program - Wa-ter) (Gilgen et al., 1998). The data was quality controlled using six separate procedures (checking of physical probability, time series analysis and comparison of cloud data). Temperature, humidity, wind data, sunshine duration and days with rain were taken from WMO Climatological Normals

1961–1990 (WMO, 1998). To replace missing data and ensure a homogeneous distribution of weather stations, other databases such as the data summary of international weather stations compiled by the National Climatic Data Center, USA (NCDC, 1995/2002) were added. For some stations in the USA, monthly mean values 1961–1990 of global radiation of the National Renewable Energy Laboratory (NREL) database "The Solar Radiation Data Manual For Buildings" were used.

For version 7.0 six data sources were updated:

- Swiss database (based on Swissmetnet of MeteoSwiss): The main period for radiation was ex-tended to 1986–2005 for radiation and to 2000–2009 for temperature, wind and precipitation.
- Globalsod data (NCDC, 2002): The parameters temperature, wind speed (10 m above ground) and precipitation were processed to 2000–2009 means.
- GEBA: The main period was extended to 1986–2005.
- Turkish State Meteorological Service: 9 stations with global radiation from 2004–2013 were add-ed.
- NREL: Monthly means of selected TMY3 sites (those within the lowest uncertainty class) were added.

The monthly average radiation values were calculated for periods of at least 10 years. Although the 10-year periods differ between the stations, a uniform period was used for each continent. For some stations the data was extended with data from neighboring stations using a differential procedure. The database contains **a total of 8'275 weather stations**.

(B) Satellite data:

In this version (version 7.1) satellite data is used for radiation interpolation in remote areas Figure (). Where no radiation measurement is available nearer than 200 km (Europe: 50 km) from the selected location, satellite information is used. If the nearest site is more than 30 km (Europe: 10 km) away, a mixture of ground and satellite information is used.

The method used for processing the satellite images is an approximation of methods like Heliosat II (Lefebvre et al., 2002): The 3 hourly pictures of the visible channel of the 5 geostationary satellites have been used (period 2009-2014). The

satellite pictures are processed to daily means of global radiation and summed up to monthly values. These monthly values are interpolated with mean ground measurements (mainly GEBA data). The difference between the ground measurements and satellite information is interpolated spatially with the inverse distance method. This provides a result which includes the values at the ground stations and the variation of the satellite pictures, for Africa data for the period 986-2005 from CMSAF4 (DWD) is used [Meteonorm software v.7.1 handbook part one, 2014].

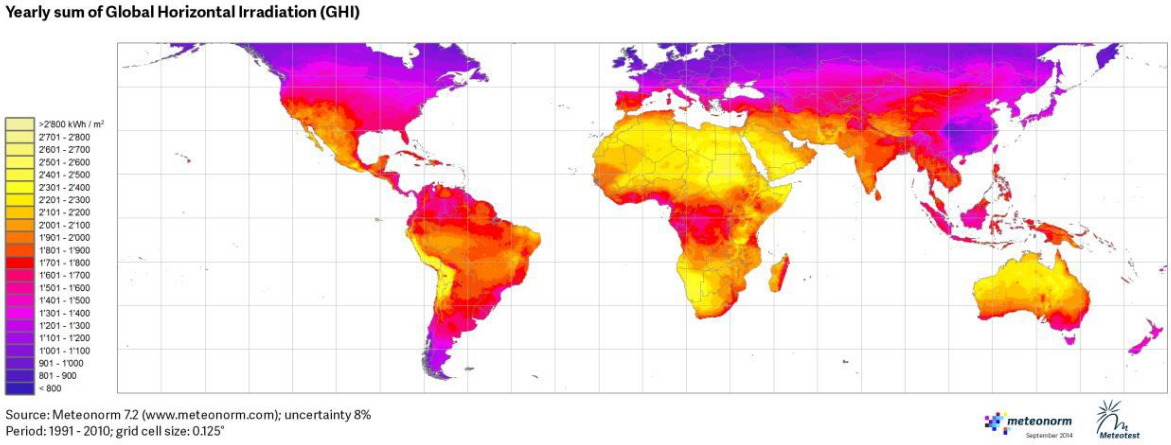

Figure(3.3): Map of yearly sum of global irradiation in kWh/m² based on satellite and ground information. Means adapted mainly to the period 1991–2010[Meteonorm software v.7.1 handbook part one, 2014].

Section two:

Reservoir simulation and Performance study:

3.3.1. Operating Scenario:

Three operating scenario have been proposed to introduce solar steam generation system as an alternative to the conventional steam generator (once through steam generator (OTSG)), each scenario requires a different type of facilities and equipments, which has a different dependency level on solar energy and variation of injection hours per day. However, no specific design aspects were discussed for the steam generating system in any scenario

All of these scenarios were modified to provide the same cumulative steam to be injected at the end of the studied period, where each scenario has a different steam injection rate based on the general steam generating system configuration.

The effect of implementing each scenario on the performance of the steam flooding pilot was studied using a commercial reservoir simulation software (CMG), the effect on the performance will be study by comparing the result of the simulation in each scenario with simulation result of the designed case that have been implemented at the field (Case 6) As discussed in chapter 2 [Husham Elbaloula et al, 2016].

The effect of implementing each scenario on the performance of the pilot is measured in term of the following parameters:

1. Cumulative oil produced (STB).
2. Cumulative water produced (STB).
3. Cumulative oil steam ratio(BLL/BLL)
4. Oil recovery (%)
5. Overall field water cut (%).
6. Oil Rate (STB/day).
7. Wells BHP
8. Break through times.

3.3.1.1. The 100% Solar Steam Generation:

This scenario depends mainly on solar energy to generate all the required steam for the project. To depend on solar energy has the advantage of reducing the volatility of

field operating costs as the cost of steam generated is independent of the cost and availability of natural gas. Moreover, it also secures the long term cost of steam once the system is installed since solar steam generators can produce at low operations cost [Mark Gregory, 2014].

One of the main concerns when depending upon solar energy only is the weather condition and change in seasons during the year, which may affect the performance negatively and result in down time during year.

Operation aspects:

Theoretically, in this scenario we assume the solar field would operate continuously for twelve hours per day (according to the average daylight hours in SSE (NASA) at field location = 12.6 hour). Practically, this may be possible when using a Thermal Storage unit that not only allow to storage the thermal energy to extend the injection period but also overcome any fluctuations in steam output associated with short-term disturbances such as passing clouds [Massachusetts Institute of Technology2015]

The twelve hour injection was assumed to reduce the required daily injection rate in order to obtain the same cumulative steam to be injected at the end of the study period. Hence, the injection rate in case of twelve hours injection should be twice the rate in continues steam injection, while it should be higher than the continues injection by a factor of 2.4 (24/10 h) if the injection were only conduct for a 10 hours per day.[Antoon Peter van Heel.2010]

3.3.1.2. The Solar Steam Generation with a Long-term Thermal Storage backup:

Concentrating Solar Power (CSP) technologies capture the solar energy as heat providing the opportunity to store this heat for a period of time using different type of thermal storage units.

The energy storage capacity of CSP plant can be expressed in term of number of hours that the plant can operate at its design capacity using only the storage system. For example, thermal storage of six hours means that the CSP plant can operate for six hours at its nameplate capacity using only the thermal energy from the storage

system (with no energy from the solar field) [Massachusetts Institute of Technology2015]

This scenario point out the role of using a long term thermal storage units to increase the injection hours per day, hence provide a lower injection rate to obtain the same cumulative steam to be injected, and provide more flexibility to the required reservoir injectivity. However, the thermal energy storage system should be designed carefully to match the required steam properties and the main thermal EOR and Oil industry objectives which is very different from electricity generation.

Of course, adding thermal energy storage to a CSP plant is not free. Additional capital and operating costs are incurred above and beyond those that would accompany a facility without storage [Massachusetts Institute of Technology2015], As a result, decisions about whether to add storage to a CSP system become questions of a techno-economic optimization.

Operation aspects:

In this scenario, the injection was assumed to continue for additional 6 hours as compare to the first scenario, during which the injected steam was generated from the storage system. Which means the injection continue for 18 hours per day (depending on solar energy and the energy obtained from thermal storage units) and the required injection rate is higher by a factor of 1.333 (24/18) than the rate used in the 24 hours continues steam injection (the rate of the conventional steam generator) to obtain the same cumulative steam to be injected.

3.3.1.3. Solar Steam generation with Natural Gas Backup:

This scenario was proposed to overcome any possible concerns related to the weather effect in the operation, it's include using natural gas boilers as backup for down weather and nightly injection in a hybrid system, such scenario though it used natural gas, but it provide less independency on fuel price and less harmful to the environment compare to the conventional steam flooding.

Operation aspects:

Since the injection rate and period stays the same as in the conventional steam flooding, from reservoir simulation point of view the output will remain the same, considering any possible reduction in the solar steam generated is covered by the once through system so that the injection rate remain constant and continues as designed. In the other hand the economical aspect can be much different.

3.3.2. CMG STARS Reservoir Simulation Software:

All reservoir simulation discussed in the research was done by Computer Modeling Group (CMG) STARS commercial software (Steam, Thermal and Advanced processes Reservoir Simulator).

STARS is a thermal, K-value compositional, chemical reaction and geomechanics reservoir simulator ideally suited for advance modeling of recovery processes involving the injection of steam, solvents, air and chemicals [CMG website].

The equations solved by CMG STAR software are divided into the following:

1. Conservation equations.

2. Phase Equilibrium Relationships.

3. Well Equations.

These equations are the result of expressing all the relevant physical phenomena in mathematical form. There is one conservation equation for each chemical component for which a separate accounting is desired, along with some equations describing phase equilibrium between phases. There exists a set of these equations for each region of interest, which is usually a discretized grid block. Lastly, there is an equation describing the operating condition of each injection and production well.

3.3.2.1. Conservation Equations:

A conservation equation is constructed for each component of a set of identifiable chemical components that completely describe all the fluids of interest.

All conservation equations are based on a region of interest (with volume V) in which:

rate of change of accumulation

= net rate of inflow from adjacent regions + net rate of addition from sources and sinks

Each of these three terms will be considered separately, below.

3.3.2.1.1. Accumulation Terms:

The total gross volume of a grid block may be composed of the following:

$$V = Vr + Vs + Vw + Vo + Vg \quad (3.1)$$

$$Vf = Vw + Vo + Vg \quad (3.2)$$

$$Vv = V - Vr = Vf + Vs \quad (3.3)$$

$$\phi v = \frac{Vv}{V} \quad (3.4)$$

$$\phi f = \frac{Vf}{V} = \frac{(Vv - Vs)}{V} = \left(\frac{Vv}{V}\right) \bullet \left(1 - \frac{Vs}{Vv}\right) \quad (3.5)$$

Where:

- solid (inert) rock matrix (r)
- solid and adsorbed component (s)
- water or aqueous phase (w)
- oil or oleic phase (o)
- gaseous phase (g)
- total volume (V)
- fluid volume (Vf)
- void volume (Vv)
- Void porosity (ϕv)
- Fluid porosity (ϕf)

If we substitute the definition of ϕv, and recognize that (Vs/Vv), the fraction of void volumeoccupied by solid and adsorbed components together is equal to Σ csi/ρsi, then:

$$\phi f = \phi v \bullet (1 - \Sigma csi / \rho si) \quad (3.6)$$

Note that if there is no solid or adsorbed component, then csi = 0 and Vs = 0, making Vv = Vfand ϕv = ϕf.

3.3.2.1.2. The saturations are defined as:

$Sw = Vw/Vf = Vw/\phi f V$,

$So = Vo/Vf = Vo/\phi f V$, and

$Sg = Vg/Vf = Vg/\phi f V$, so that

$$Sw + So + Sg = 1 \qquad (3.7)$$

The accumulation term for a flowing and adsorbed component i is

$$\frac{\partial}{\partial t}[Vf(\rho wSwWi + \rho oSoXi + \rho gSgYi) + VvAdi] \qquad (3.8)$$

The accumulation term for solid component is:

$$\frac{\partial}{\partial t}[VvCi] \qquad (3.9)$$

The accumulation term for energy is:

$$\frac{\partial}{\partial t}[Vf(\rho wSwUw + \rho oSoUo + \rho gSgUg) + VvCsUs + VrUr] \qquad (3.10)$$

Here Uj, j=w,o,g,s

are the internal energies as a function of temperature and phase composition, and ρj, j = w, o, g

are fluid phase densities. Ur is energy per rock volume, and cs is total solid concentration

3.3.2.1.3. Flow Terms:

Well source/sink terms are the means by which all the thermal EOR processes are driven. The flow term of flowing component I between two regions is

$$\rho wV\ wWi+\rho oVoXi+\rho gVgYi+\Phi\rho wDwi\Delta wi+\Phi\rho gDgi\Delta Yi+\Phi\rho oDoi\Delta Xi$$

Solid components have no flow terms.

The flow term of energy between two regions is

$$\rho_w V_w H_w+\rho_o V_o H_o+\rho_g V_g H_g+K\Delta \qquad (3.12)$$

The volumetric flow rates are:

$$Vj=T\left(\frac{Krj}{\mu jrj}\right)\Delta\Phi jj=w,o,g \qquad (3.13)$$

Where:

T is the transmissibility between the two regions.

Dji (j=w,o,g) are the component dispersibilities.

K is the thermal transmissibility at the interface between the two regions

The potential at a grid node is Φj = pj - λjgh. The potential difference ΔΦjis the value at the node of the adjacent region minus the value at the node of the current region of interest. A positive value for ΔΦj represents inflow, a negative value gives outflow. The concentration differences Δwi, Δxi, Δyi are the differences in phase concentrations between the nodes, following the same sign convention as ΔΦ. If a phase is not present in one of the adjacent blocks, the concentration difference is set to zero (no dispersive transport).

ΔT is the temperature drop between the nodes, again following the same sign conventionas ΔΦ.

3.3.2.1.5. Well Source/Sink Terms

Well source/sink terms are the means by which all the thermal EOR processes are driven.

The well source/sink term for flowing component i is

$$\rho w\, qwk\, wi + \rho o\, qok\, xi + \rho g\, qgk\, yi \qquad (3.14)$$

Solid components have no well terms.

The well source/sink term for energy is

$$\rho w\, qwk\, Hw + \rho o\, qok\, Ho + \rho g\, qgk\, Hg \qquad (3.15)$$

Note the similarity between these terms and the interblock flow terms discussed above. The volumetric flow rate q is analogous to V, but is calculated very differently.

The well phase rates are

$$qjk = Ijk \bullet (pwfk - pk)\ j=w,o,g \qquad (3.16)$$

Where:

Ijk is the phase j index for well layer k

pk is the node pressure of the region of interest which contains well layer k.

pwfk is the flowing wellbore pressure in well layer k.

3.3.2.1.6. Chemical Reaction and Interphase Mass Transfer Source/Sink Terms:

The reaction source/sink term for component i is:

$$V \sum_{k=1}^{nr} (S'ki - Ski).rk \qquad (3.17)$$

And the reaction source/sink term for energy is:

$$V \sum_{k=1}^{nr} Hrk\, rk \qquad (3.18)$$

Where:

S'ki is the product stoichiometric coefficient of component I in reaction k.

Ski is the reactant stoichiometric coefficient of component I in reaction k.

Hrk is the enthalpy of reaction k.

rk is the volumetric rate of reaction k, calculated from a model for reaction kinetics.

3.3.2.1.7. Heat Loss Source/Sink Terms:

The heat loss source/sink term for energy is

$$\sum_{k=1}^{nr} HLk + HLv + HLc \qquad (3.19)$$

Where:

HLk is the rate of heat transfer to the region of interest through block face number k, from the adjacent formation. The heat transfer rate and heat accumulated in the overburden are calculated using an analytical solution for an infinite overburden. Heat flow back into the reservoir block may occur.

HLv is the rate of heat transfer calculated from a convective model.

HLc represents a constant heat transfer model.

3.3.2.1.8. Thermal Aquifer Source/Sink Terms:

The aquifer source/sink term for water component is:

$$\sum_{k=1}^{nf} \rho w q_a q_w k \qquad (3.20)$$

And for the energy:

$$\sum_{k=1}^{nf} (HAcv + HAcD)_k \qquad (3.21)$$

Where:

$\square a \square w$ is a volumetric water flow rate through a block face k to/from the adjacent aquifer.

HAcv is a rate of heat transferred by convection to/from the adjacent aquifer.

HA_{CD} is a rate of heat transferred by conduction to/from the adjacent aquifer.

All flow rates are calculated using a semi-analytical model with various boundary conditions

3.3.2.2. Phase Equilibrium Relationships:

The phase mole fractions are related by the equilibrium ratios, or K values:

$$Yi = Kigo\, Xi \quad ; \quad Xi = Kiog\, Yi$$

$$Xi = Kiow\, Wi \quad ; \quad Wi = Kiwo\, Xi$$

$$Wi = Kiwg\, Yi \quad ; \quad Yi = Kigw\, Wi$$

$$\sum_{i=1}^{nc} Yi = 1 \; when \; Sg > 0 \qquad (3.22)$$

$$\sum_{i=1}^{nc} Xi = 1 \; when \; So > 0 \qquad (3.23)$$

$$\sum_{i=1}^{nc} Wi = 1 \; when \; Sw > 0 \qquad (3.24)$$

The phase pressures and saturations are constrained by:

$$Sw + So + Sg = 1 \qquad (3.25)$$

$$Pw = Po - Pcow(sw) \qquad (3.26)$$

$$Pg = Po + Pcog(Sg) \qquad (3.27)$$

3.3.2.3. Well Equations:

Simple single-block wells may be characterized with a constant rate or pressure, but a fullycoupled treatment of a well completed in several blocks requires a more

comprehensive approach. Each equation listed below represents a well operating condition, and exactly one equation per active well is in force at any one time.

The following, the subscript “spec” indicates a quantity specified by the user as an operating condition. These equations apply to both injection and production wells.

a. Constant Pressure:

$$p_{wf} = p_{spec} \tag{3.28}$$

This is the simplest well equation. Rates are calculated, and can be checked against auxiliary operating constraints.

b.Constant Water Rate:

$$\sum_{k=1}^{nlay} q_{wk} = q_{spec} \tag{3.29}$$

This is solved simultaneously with the conservation equations, with pwf as an additional variable. Even though qspec is constant, the distribution of water to different layers depends on Ijk which can change with time.

3.3.2.3.3. Constant Oil Rate:

$$\sum_{k=1}^{nlay} q_{ok} = q_{spec} \tag{3.30}$$

3.3.2.3.4. Constant Gas Rate:

$$\sum_{k=1}^{nlay} q_{gk} = qspec \tag{3.31}$$

3.3.2.3.5. Constant Liquid rate:

$$\sum_{k=1}^{n_{lay}} (q_{wk} + q_{ok}) = q_{spec} \qquad (3.32)$$

3.3.2.3.6. Constant Steam Production Rate:

$$\frac{1}{\rho_w^{ST}} \left(\sum_{k=1}^{n_{lay}} q_{gk} Y_1 \rho_g \right) = q_{spec} \qquad (3.33)$$

Where y1 and ρg are values from the grid block containing well layer k.

The wellbore pressure pwfk at each layer is obtained by adding pwf(at k=1) the accumulated fluid head.

$$P_{wfk} = p_{wf} + \int_{h_1}^{h_k} \gamma_{av} g \, dh \qquad (3.34)$$

Section three:

3.4. The Effect of change in Seasons on the Preformance:

As discuss in the first part of the research, Solar Radiation at FNE oilfield location was compared with Amal oilfield in Oman to study the field potential to deploy concentrating solar power systems. However, Amal oilfield is location has a very low seasonal variation in sunshine [Daniel Plamer et al, 2013], While the seasonal variation in FNE location shows more significant effect and should considered.

In this research an attempt to address the effect of the seasonal variation in the performance in term of the same parameters discussed in the operating scenarios using CMG reservoir simulation software. And in order to achieve that, two approaches were proposed, both of them relate the solar radiation (DNI) data at field location with steam generated from the solar field focusing only on the steam injection rate assuming that the solar steam generating system will continue operate daily through the year and the steam injection rate is the only affected parameter by the seasonal variation.

Therefore, it's important to emphasis that these two approaches are ONLY used to discuss consequences of the variation in steam injection rate values as a result of the seasonal variation on the mention parameters, and they do not aim to forecast the actual performance of the solar steam generating system at the field location.

3.4.1. First Approach:

This approach depends on the method used by Van Heel et al in their study of the impact of daily and seasonal cycle in Solar-Generated Steam on oil recovery, where they developed an analytical "*representative*" model to perform their study at a specified condition.

To study the seasonal variation, the authors assumed a solar steam rate profile where the solar generated steam rate is modeled by an oscillation function that has an amplitude that is 25% of the yearly average steam rate, as shown in the following figure (figure ())[A.P.G. van Heel et al, 2010] (more details about the study is discussed in Chapter 2, literature review section).

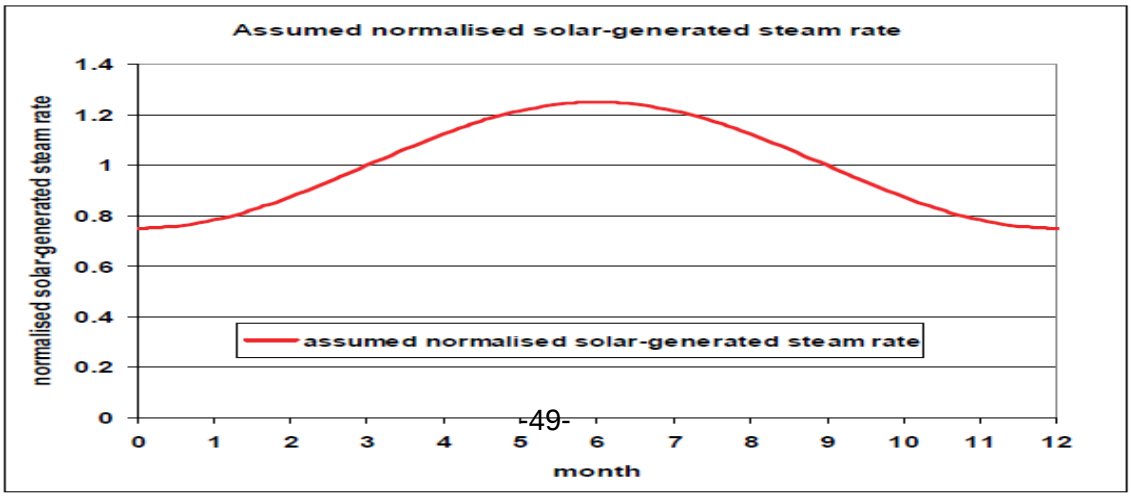

Figure (3.4): Assumed solar steam rate (seasonal variation) [A.P.G. van Heel et al, 2010].

In our simulation instead of modeling by the same function, we attempt to relate the solar steam rate profile with the solar radiation data (average DNI data) at the field location, assuming that the solar generated steam rate will increase by 25% during the months with high solar radiation and decrease by 25% during the months with low solar radiation.

This approach by the mentioned procedure will used to study the effect of seasonal variation on the first and second operating scenarios performance (100% solar scenario and 100% solar with thermal storage backup scenario), while in the last scenario the seasonal variation will not have any effect on the steam injection rate since all decrease on the steam rate will be covered by conventional steam generator system.

3.4.2. Second Approach:

The Idea behind this approach obtained from the method used to forecast the performance of the Solar EOR system deployed in Amal oilfield. Where a performance model is used to forecast solar field output (in term of tons of steam per day) based on Direct Normal Irradiation (DNI) driven from an on-site meteorological station.

However, since this research didn't present any specific design for the solar steam generation system. We assume that variation in the DNI values result in an equivalent change in the steam injection rate, hence, any increase on decrease in the average DNI value result in an equivalent increase or decrease in the steam injection rate (i.e. the solar steam rate profile will be similar to the average DNI profile).

Also this approach will be used in the first and second scenario, and as mention this approach is not used to forecast the actual performance of the solar steam

generating system at the field location, only to discuss consequences of the variation in steam injection rate values as a result of the seasonal variation on the mention parameters.

Section Four:

Highlights on the Economical and Environmental Impact

3.4.1. Fuel gas consumption:

The research use actual data obtained from Central Field Process (CPF) report, to determine the actual amount of Fuel gas feed to the Steam Generation Units (SGU). These amounts represent the total gas savings when deploying

4.4.1. Cost of Fuel:

The cost associated with natural gas consumption was calculated using the natural gas price at the time writing the research (which is equal 3.22$/scf at 2016/10/12). The calculation emphasis the significant operation cost associated with using natural gas generator when compared with low operating costs when depending on solar energy.

4.4.2. Environmental impact:

Using solar energy as a replacement of natural gas for thermal EOR has an obvious environmental impact in term of reducing the emissions of CO2, NOx and CH_4 . and other greenhouse gases. And in order to demonstrate this environmental impact in a measurable manner calculation for the amount of different greenhouse gases (GHG) emission was made based on estimated factors for different greenhouse gases (GHG) emission (at different units) published by Intergovernmental Panel on Climate Change (IPCC).

Chapter Four

Results and Discussion

Section one:

Solar Radiation and Meteorological Data

4.1.1. Solar Potential at Fula North East (FNE) Field Location:

The Average Direct Normal Irradiation (DNI) values at Fula north east (FNE) field – at the exact location of injector coordinates (Latitude **11.374** / Longitude **28.525**) – was obtained from different solar radiation database to demonstrate the solar potential at the field.

I.

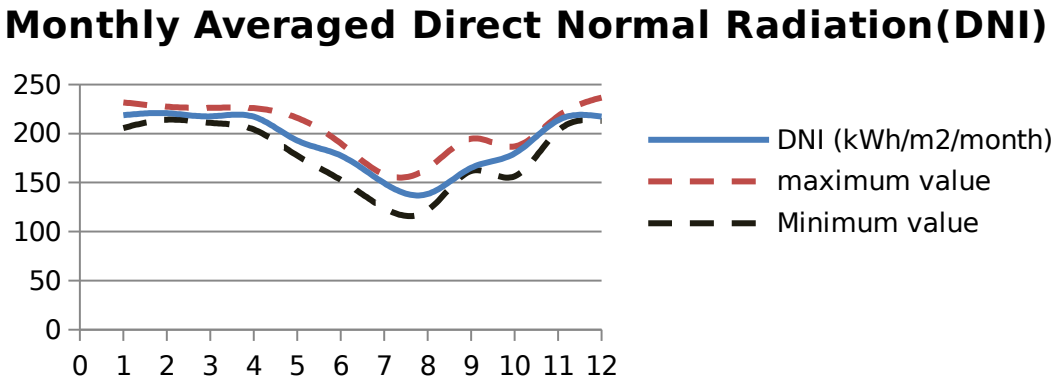

Using NASA Surface Meteorology and Solar Energy (SSE) database,

Figure (4.1)

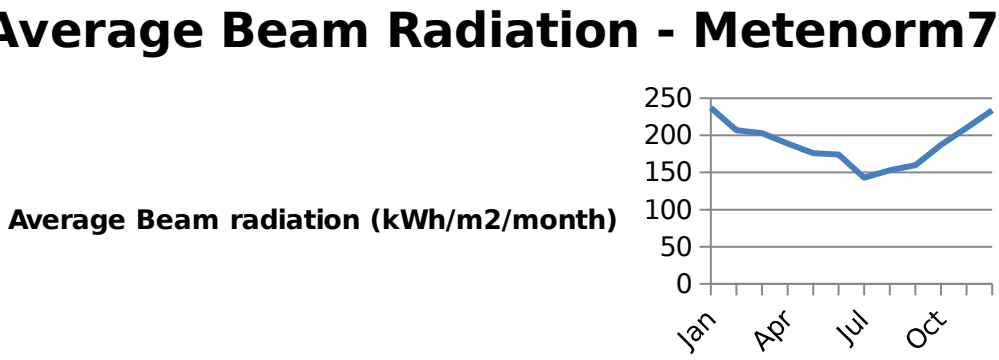

II.

Using Metronome7 meteorological database

Figure (4.2)

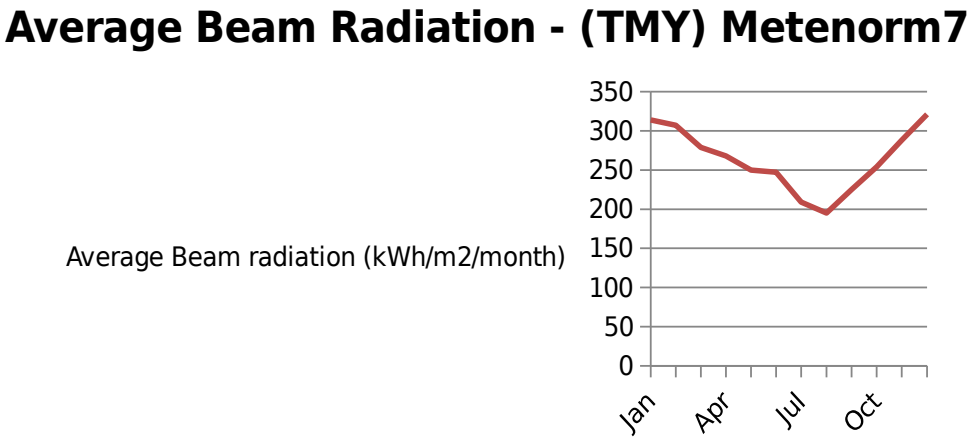

III. **Us**

ing Typical Meteorological Year data (TMY3) created by Meteonorm7 Software

Figure (4.3)

All of the above figures (from different source of database) show sufficient monthly average DNI values, with an observed reduction in the DNI starting from middle of MAY to its lowest degree in August which indicates summer autumn cycle.

4.1.2 Comparisons Solar Radiation and Meteorological parameters between FNE and Amal oilfields location:

The investigating of FNE oilfield compatibility to Concentrating Solar Power (CSP) applications was supported by comparing solar radiation and meteorological data in field location with existing solar thermal EOR project at Amal field in Southern Oman.

The first comparison is conducted between Amal model year and FNE monthly average DNI obtained from Typical Meteorological Year data (TMY3) which generated using Metenorm7 software (Figure 4.4).

The comparison made using surface (SSE) and Meteonorm7 software at FNE and Amal coordinates, and the comparison includes the following solar radiation and meteorological parameters:

- Monthly Average Direct Normal Irradiation (DNI)
- Monthly Averaged Air Temperature.
- Monthly Averaged Relative Humidity
- Monthly Averaged Wind Speed.
- Precipitation.

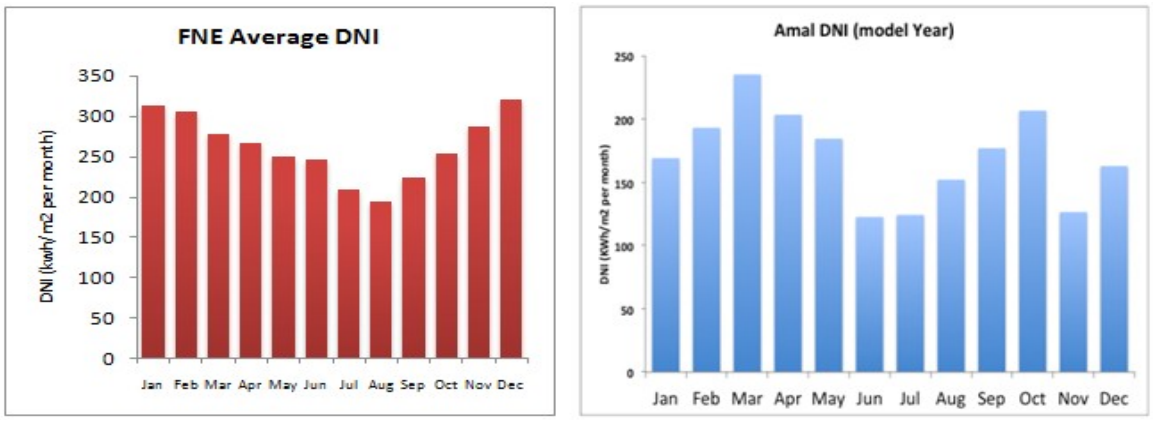

Figure (4.4)

4.1.2.1. Surface Meteorology and Solar Energy (SSE) (NASA) Data:

Surface Meteorology and Solar Energy (SSE) -Release 6.0- is a renewable energy resource web site, provides meteorology and solar radiation data obtained from the NASA Science Mission Directorate's satellite and re-analysis research programs. And the coverage of the solar and meteorological data includes more than 22 years data.

4.1.2.1.1. Input Data:

- Fields Coordinates:

1)FNE Field Coordinates: Latitude **11.36** / Longitude **28.516**.
2)Amal Field Coordinates: Latitude **18.35** / Longitude **55.65**.

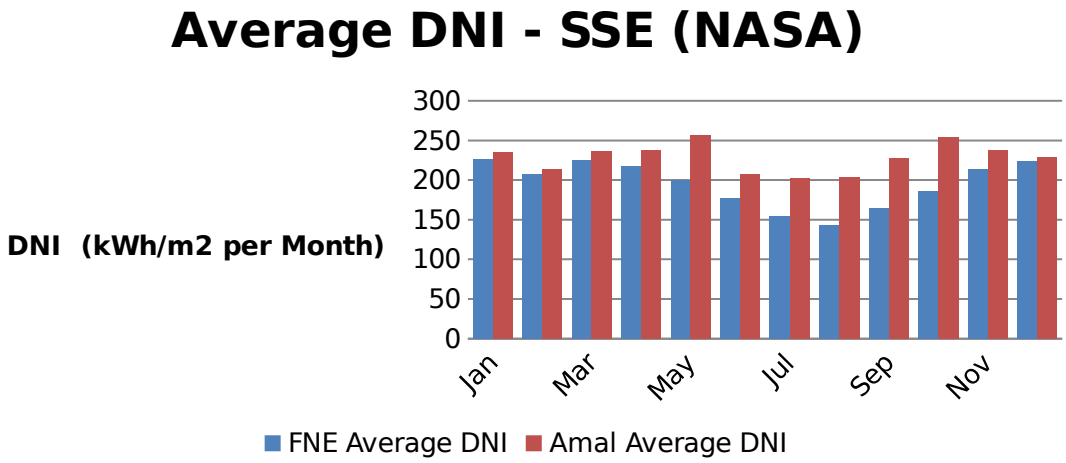

4.1.2.1.2. Monthly Averaged Direct Normal Radiation (kWh/m^2 per Month):

Figure (4.5)

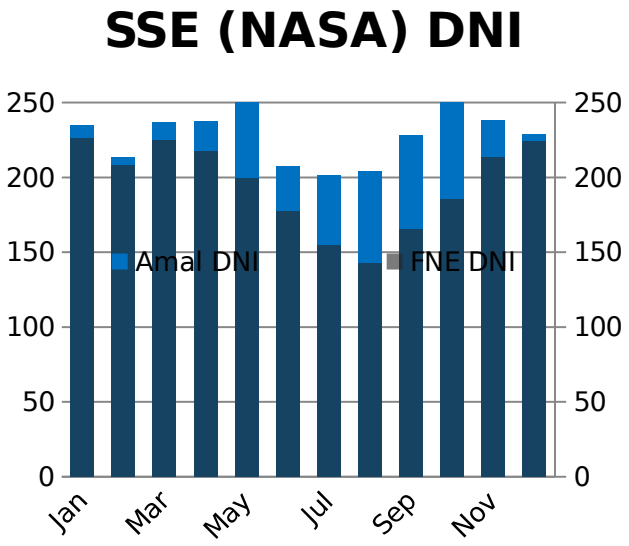

These figures shows that the Monthly average direct normal irradiation (DNI) values for Amal oilfield and FNE are very close during the period January – April and in November and December (the highest different was in November as the radiation in Amal field is higher by 24.3 kwh/m^2), while FNE average DNI decreases during the period from June to October which is a result from the seasonal effect (Autumn Season) and this seasonal variation effect on the performance and the cumulative oil produced will be discuss a head in this chapter.

4.1.2.1.3. Other Meteorological Parameters:

A. Monthly Averaged Air Temperature At 10 m Above The Surface Of The Earth (°C):

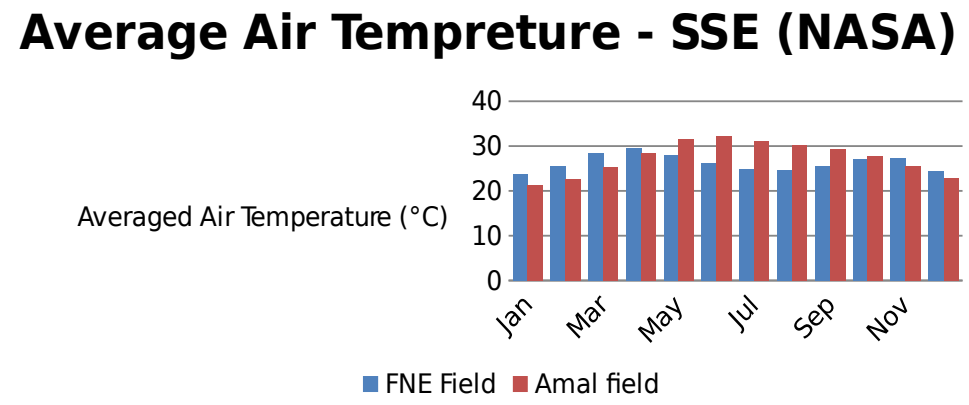

Figure (4.6)

Average air temperature near surface, show higher value at FNE field location than the values at Amal field during the period from January to April and in November and December, while seasonal variation effect also observed during the period from June to October

B. Monthly Averaged Wind Speed At 50 m Above The Surface Of The Earth (m/s):

In term of wind speed (at 50m above), FNE field location express lower values through the year, which indicate lower heat loss associated with high wind speed as in Amal field.

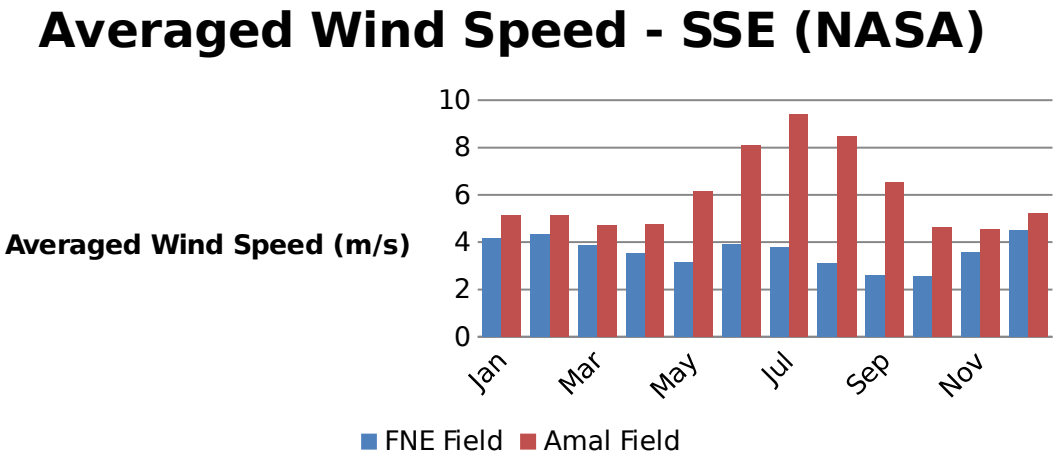

Figure (4.7)

C.

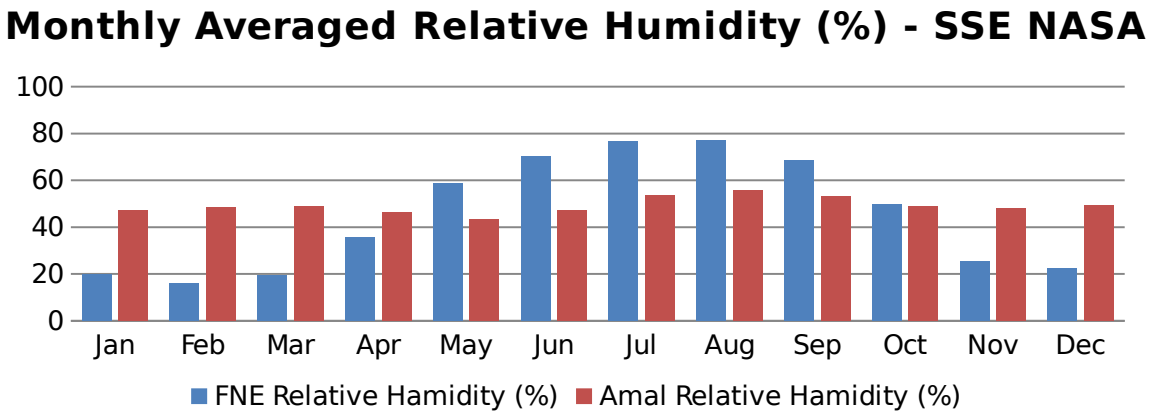

Monthly Averaged Relative Humidity (%):

Figure (4.8)

D.

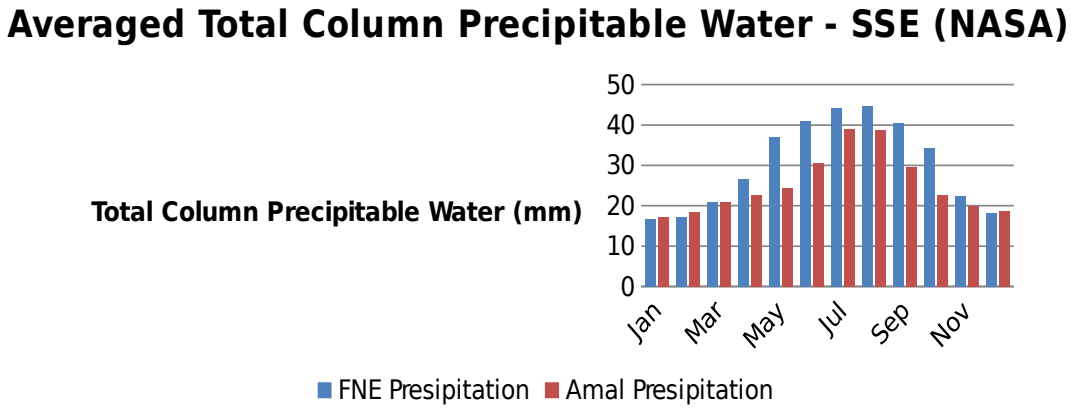

Monthly Averaged Total Column Perceptible Water (mm):

Figure (4.9)

Also as illustrate by averaged relative humidity and monthly averaged total Column Perceptible Water seasonal variation effect was also obvious during the period from June to October at FNE field location. While close values observed at Amal field during the period from January to April and in November and December.

4.1.2.1.4 Results Accuracy:

The accuracy of SSE (NASA) for both fields is summarized below (as mention in chapter 3, direct normal radiations were compared with data from BSRN and Meteorological parameters were compared with data from the NCDC):

- Table (4.1): Direct Normal Radiation

Parameter	Region	Bias (%)	RMS (%)
Direct Normal Radiation	Global	-4.06	22.73

- Table (4.2): Averaged Air Temperature & Averaged Relative Humidity:

Parameter	Slope	Intercept	R^2	RMSE	Bias

Tavg (°C)	1.02	-0.78	0.96	2.13	-0.58
RH (%)	0.79	12.72	0.56	9.40	-1.92

- Table (4.3): Averaged Wind Speed :

Parameter	Method	Bias	RMS
Wind Speed at 10 meters for terrain similar to airports (m/s)	A. RET Screen Weather Database (documented 10-m height airport sites)	-0.2	1.3
	B. RET Screen Weather Database (unknown-height airport sites)	-0.0	1.3

4.1.2.2 Meteonorm7 Data:

Meteonorm software represents a meteorological database containing climatologically data that provide method for the calculation of solar radiation on arbitrarily orientated surfaces at any desired location. The method is based on databases and algorithms coupled according to a predetermined scheme.

4.1.2.2.1. Input Data:

- Fields Coordinates:
  1) FNE Field Coordinates: Latitude **11.36** / Longitude **28.516**.
  2)Amal Field Coordinates: Latitude **18.35** / Longitude **55.65**.
- Radiation Period: 1991 – 2010
- Temperature Period: 2000 – 2009

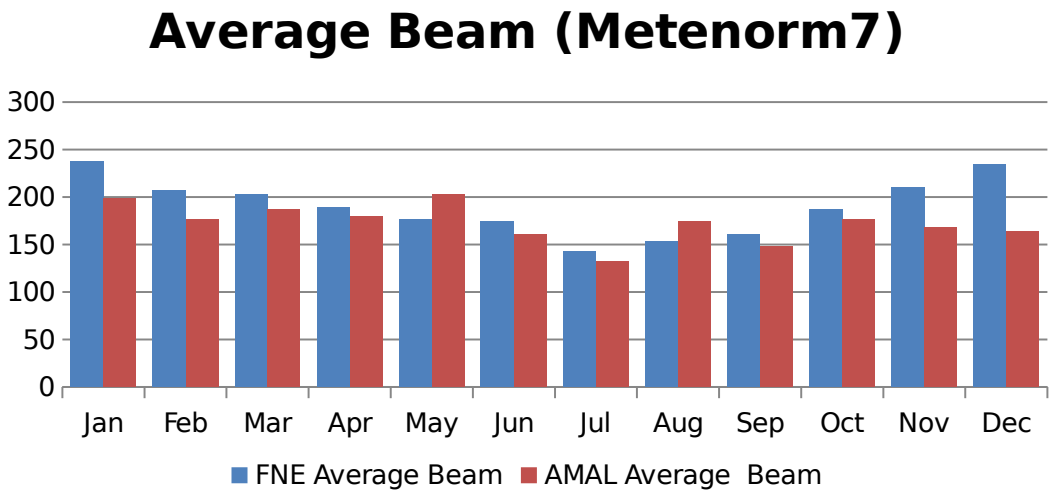

4

.1.2.2.2. Monthly Averaged Beam Radiation (kWh/m^2 per Month):

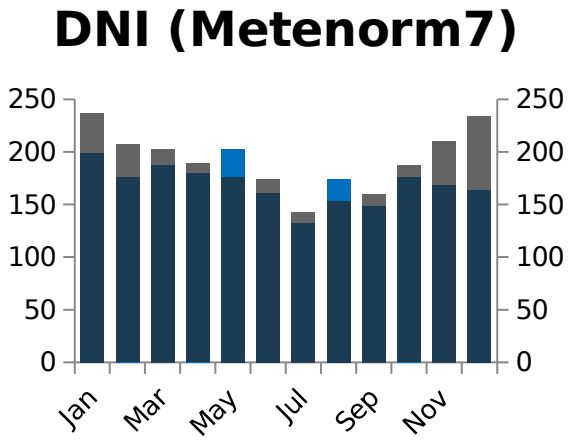

Figure (4.10)

These figures show that the Monthly average Beam radiation values obtained from Meteonorm7 for FNE oilfield exceeds Amal oilfield during most of the year except in May and August. Tough, a decrease in average Beam values is also observed during the period from June to October which is a result from the seasonal effect (Autumn Season).

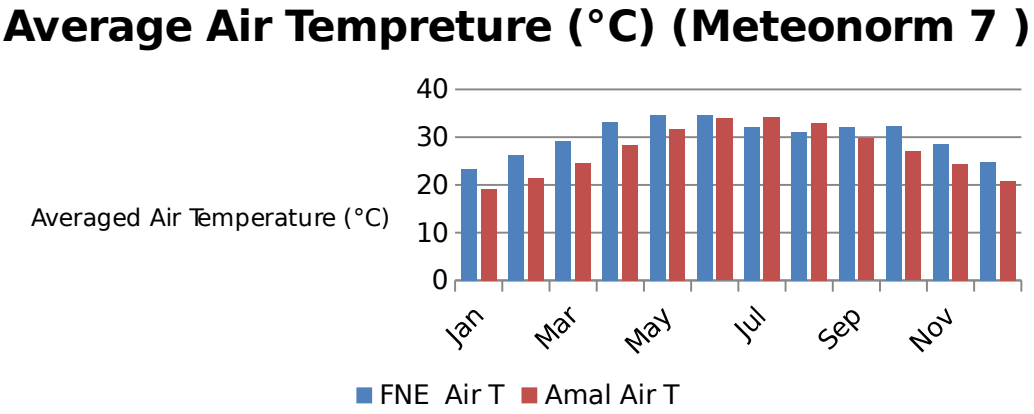

4.1.2.2.3. Other Meteorological Parameters:

A. Monthly Averaged Air Temperature At 2 m Above The Surface Of The Earth (°C):

Figure (4.11)

From the above figure, the air temperature at 10 m above the surface of the earth in FNE is higher than Amal, except during the July and August.

B.

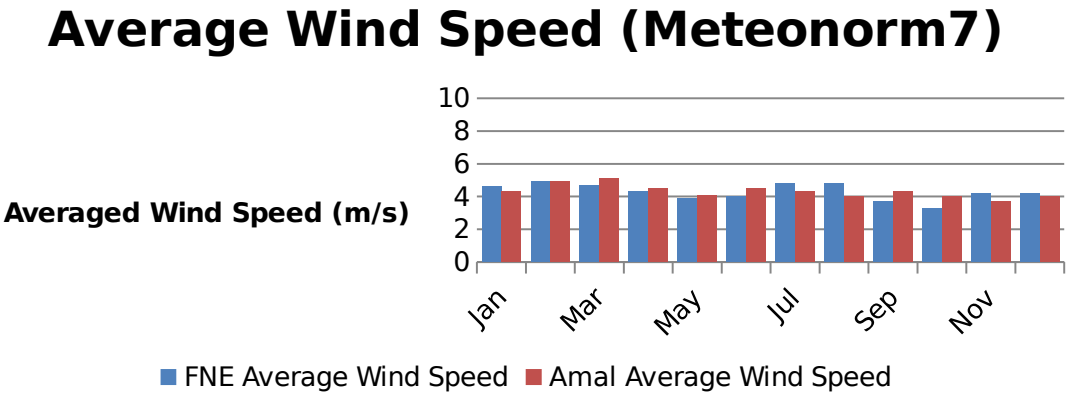

Monthly Averaged Wind Speed (m/s):

Figure (4.12)

The average wind speed data, as presented in the above figure (figure (4.11)), shows a huge similarity between the two location, with the maximum different at August of (0.8 m/s)

C. Monthly Averaged Relative Humidity (%):

The relative humidity values as shown in figure (4.12), shows high low values at FNE location compared to Amal field location, except during the autumn season as the humidity increase significantly but still the maximum value for the relative humidity of FNE field location is lower than Amal.

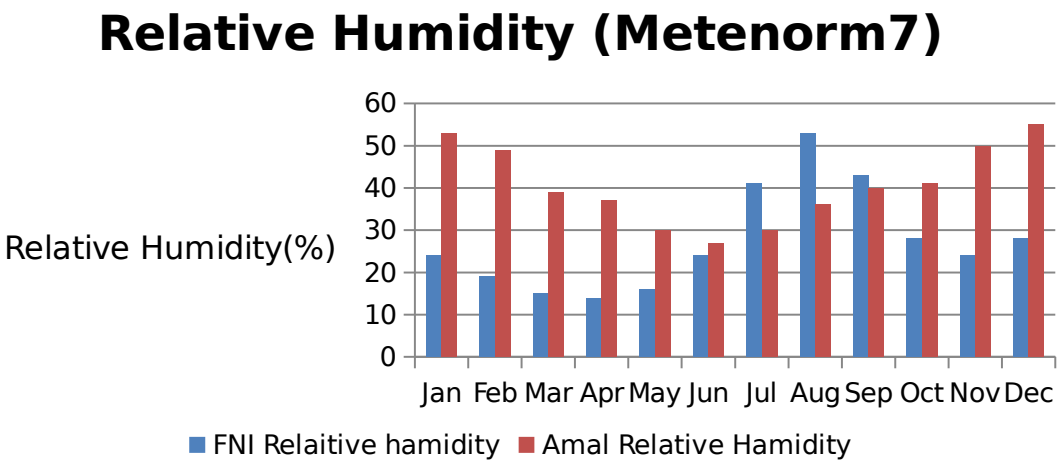

Figure (4.13)

The relative humidity values, shows high low values at FNE location compared to Amal field location, except during the autumn season as the humidity increase significantly but still the maximum value for the relative humidity of FNE field location is lower than Amal.

- At Amal field: Maximum RH = 55% in January
- At FNE field: Maximum RH = 53% in August.
-

D. Monthly Average Precipitation:

Figure (4.14): **FNE Precipitation (mm)**

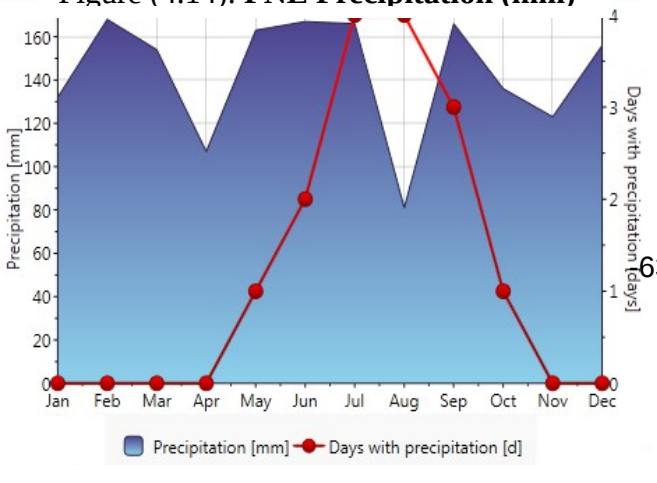

Figure (4.15): **Amal Precipitation** (mm)

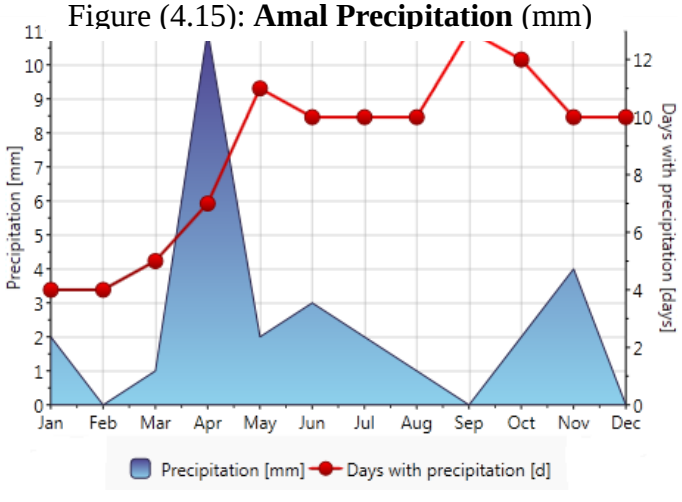

As illustrate in the figures (4.14 and 4.15), FNE field have very high precipitation when compare to Amal field. However, all precipitations are limited to specific period From May to October and within 4 days with precipitation.

4.3.2.4 Results Information and Accuracy:

FNE Oilfield

– Number of interpolation station(s):
  - ❖ Air Temperature(Ta): Only 2 station(s) for interpolation
  - ❖ Relative Humidity(Rh): Only 1 station(s) for interpolation
  - ❖ Precipitation(RR): Only 1 station(s) for interpolation
  - ❖ Wind Speed(FF): Only 1 station(s) for interpolation
  - ❖ Global Radiation, Horizental(Gh): Use of precalculated radiation map based on satellite and ground information due to low density of network.
– Nearest 3 stations: Ta: Khartoum (643 km), Ndjamena (Fort Lamy) (1472 km)
– Uncertainty of yearly values: Gh = 7%, Bn = 13 %, Ta = 2.4 °C
– Trend of Gh / decade = - %
– Variability of Gh / year = 6.1%

Amal Oilfield:

– Number of interpolation station(s):
  - ❖ Effective Sunshine Duration(SD): Only 2 station(s) for interpolation
  - ❖ Days with Precipitation (> 0.1mm)(RD): Only 3 station(s) for interpolation
  - ❖ Global Radiation, Horizental (Gh): Use of precalculated radiation map based on satellite and ground information due to low density of network.
– Nearest 3 stations: Ta: MARMUL (AUT) (55 km), THUMRAIT (OM-AFB) (188 km), Salalah (222 km)
– Uncertainty of yearly values: Gh = 12%, Bn = 23 %, Ta = 0.8 °C
– Trend of Gh / decade = -3.6%
– Variability of Gh / year = 3.2%

The comparison between the two fields' location proves the significant solar radiation potential and very acceptable meteorological data at FNE in the months from January to April, and in November and December. While seasonal effect at field location was clearly observed in term all presented solar radiation and meteorological parameters

Section two:

Reservoir Simulation and Performance Study

4.2.1 Fula North East (FNE) Reservoir Model:

A reservoir simulation model for FNE steam flooding pilot project which was obtained from literature has been run for fifteen years period with actual properties and simulation history with three cyclic steam stimulation periods, Steam injection temperature of 270 °C, with 5~7 MPa injection pressure , steam injection quality of 0.6 , pay depth 550m , pay thickness 30m ,porosity 32%,oil saturation 70% , dead oil viscosity 661m Pa.s(50°C),and reservoir pressure 610psi ; were used as steam flooding parameters for all simulation cases [Husham Elbalola et al, 2016].

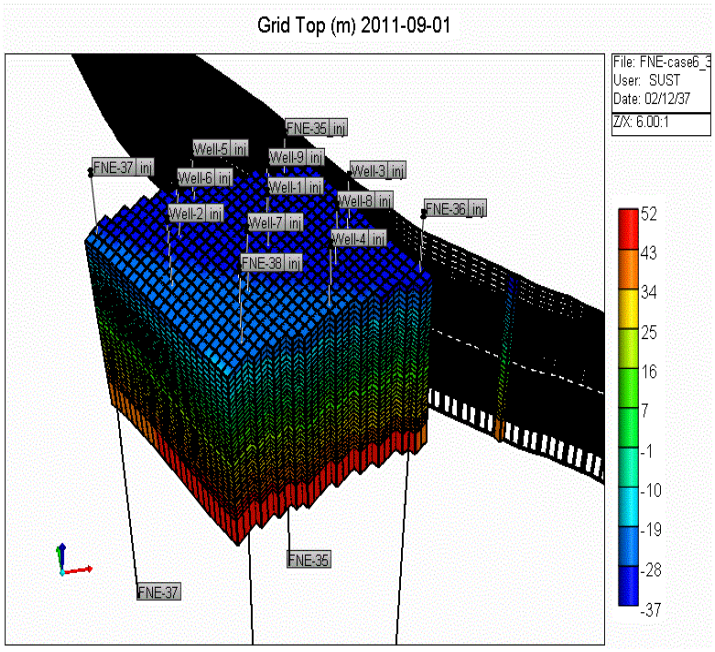

Figure (4.16)

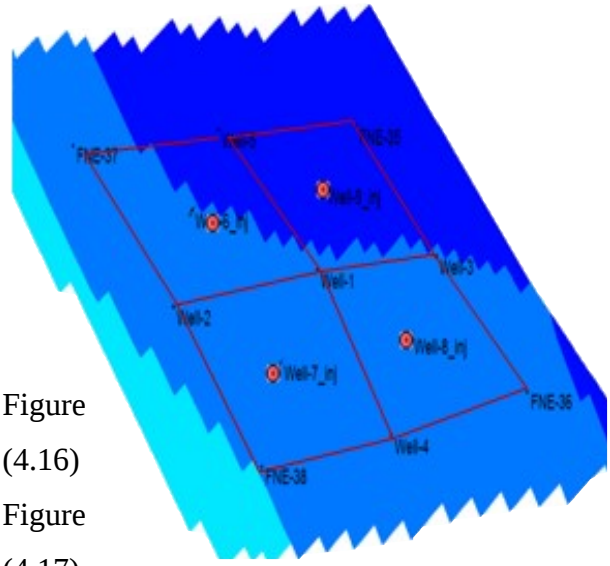

Figure (4.17)

Figure (4.17) show the project was developed as five spot injection pattern where wells (well6_inj, well7_inj, well8_inj, well9_inj) are injection well and the wells (FNE-35, FNE-36, FNE-37, FNE-38, Well-1, Well-2, Well-3, Well-4) are producers.

The model has been adjusted to adapt with the three proposed scenarios, where solar limitation to generate the required steam was considered focusing in the effect of day-night cycle in steam generation, (where the well is shut-in in the night and all the injection is during the day time) – **100% solar steam generation scenario -** and the additional steam generation provides by the thermal storages tanks – **solar steam generation with long term thermal storage tanks scenario.**

Finally, the model was re-adjusted in an attempt to discuss the effect of the seasonal variation in the performance. Where to approaches was proposed to relate the presented solar radiation (DNI) data at field location with the solar steam generation in term of steam injection rate and rate profile.

4.2.2. Reservoir Simulation Model Timeline:

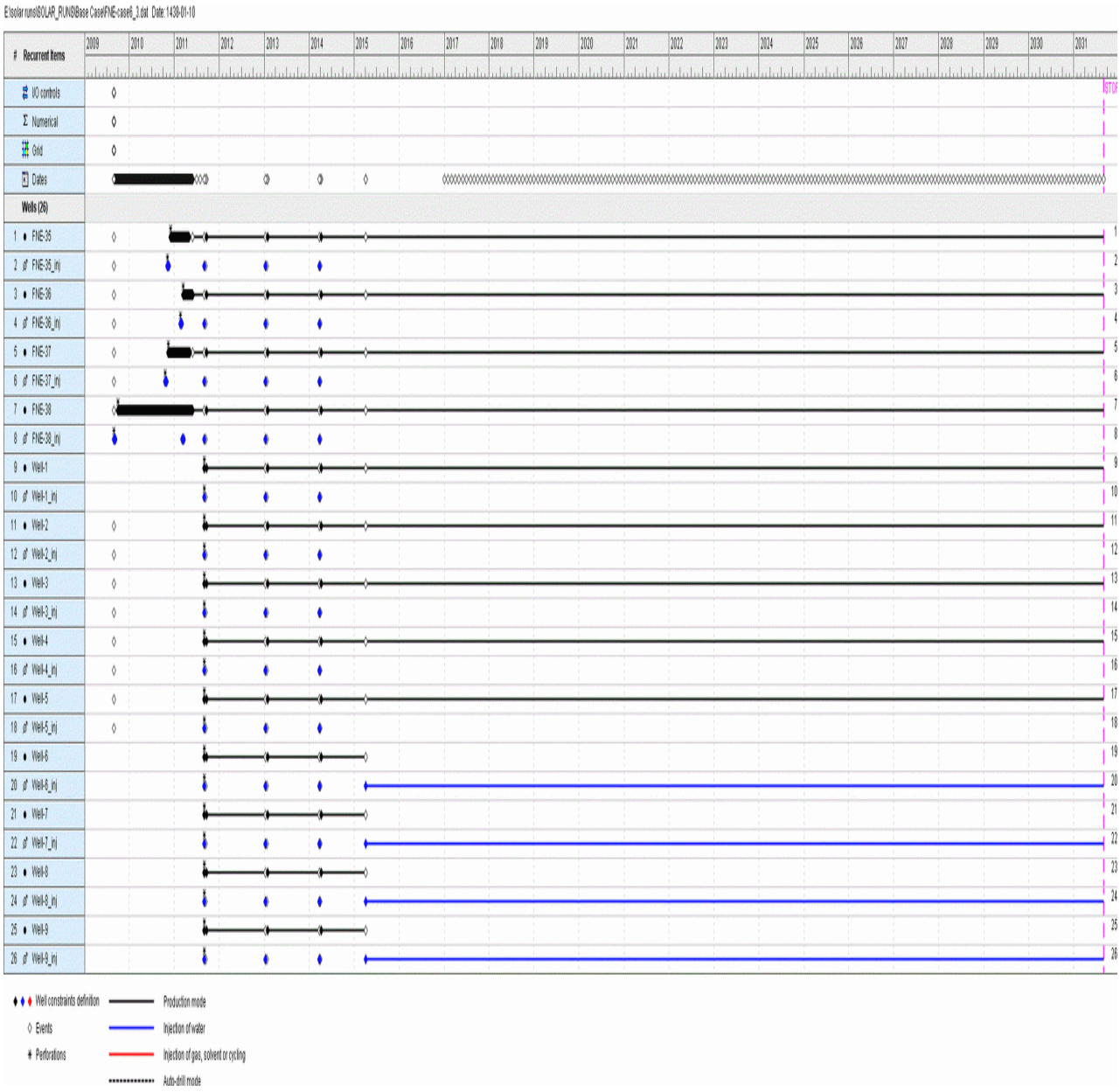

Figure (4.18)

The figure shows the events and the history of the project before the flooding begins where all wells had three cyclic stimulation periods (some wells subjected to more than three).

1.2.3 Reservoir Simulation Results:

Simulation results for all scenarios are compared with constant steam injection rate of 115m^3/day as a base case. The comparison is limited to the following parameters:

1. Cumulative oil produced (STB).
2. Cumulative water produced (STB).
3. Cumulative Oil Recovery Factor (%).
4. Cumulative Oil Steam Ratio (bbl/bbl)
5. Overall field water cut (%).
6. Oil Rate (STB/day).
7. Break through time.

8. 4.2.3.1 The 100% Solar Steam Generation:

9. This scenario depends mainly on solar energy to generate all the required steam for the project. As discuss in Chapter 3 this scenario assumed to operate continuously for 12 hours a day, and the injection rate in this scenario is twice (multiply by a factor of 2 (24/12)) the rate in base case as sown in the following finger (figure (4.18)),

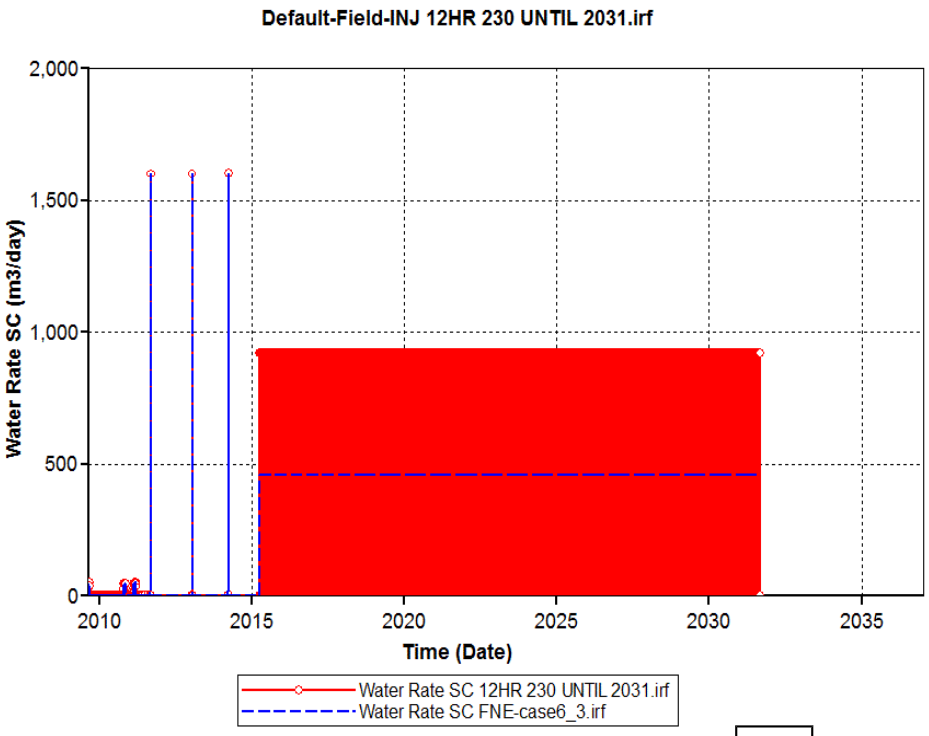

(a

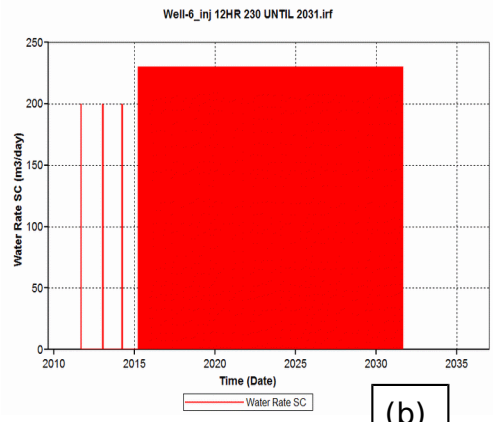

(b)

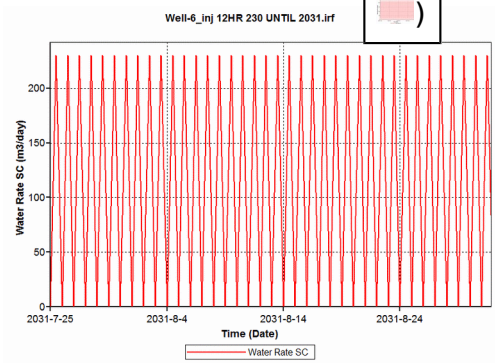

)

10. Figure (4.19)

(C

11. Figure (4.19): discribe (a) total field injection rate, (b) well 6 injector injection rat as an example. (c) closer view of well 6 injection rate.

12. Note: the red area represents daily opening and closing for the injector (the injection for 12 hours) described by figure (Figure 4.19 (c)) which represent the rate from 2031/7/25 to 2031/8/24.

A. cumulative oil production

13.

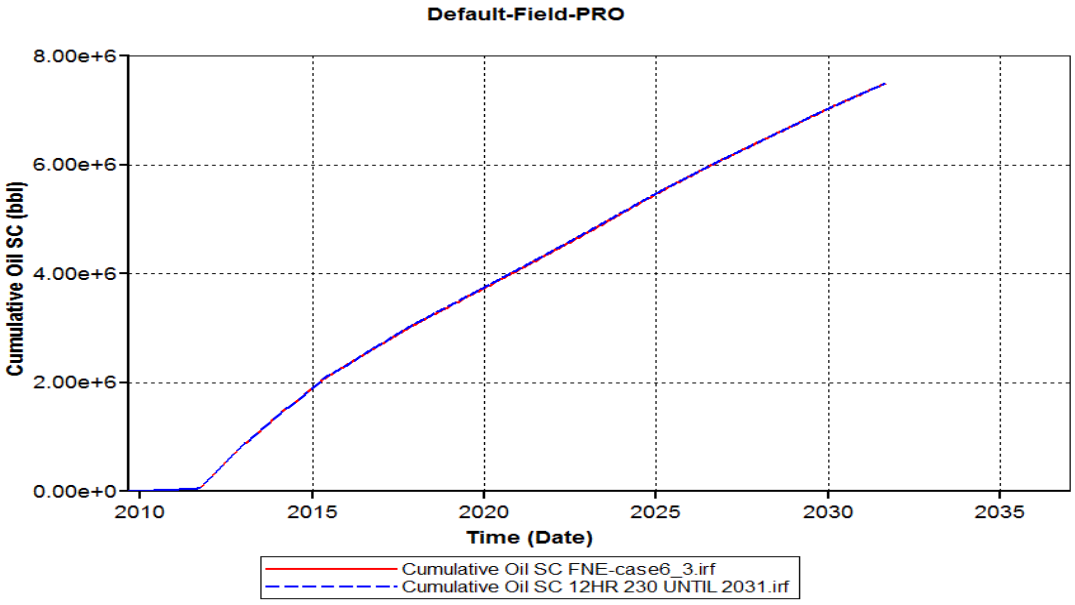

14. Figure (4.20)

A. cumulative water production

15.

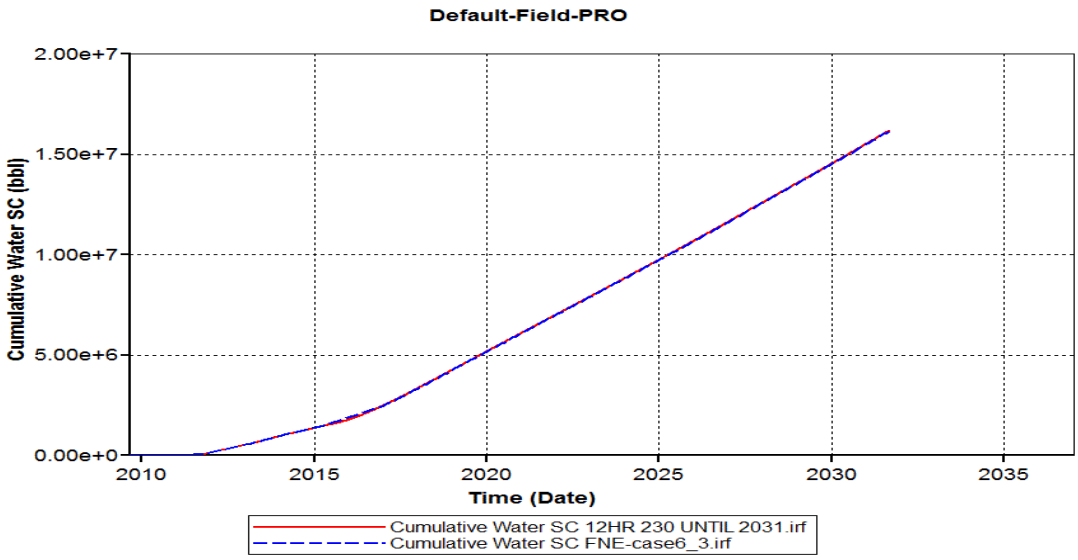

16. Figure (4.21)

17.

18. The simulation results in figure (4.20) and figure (4.21), shows that the cumulative oil production curve and cumulative water production curve for first scenario MATCH the based case curves, therefore no obvious negative effect observed.

19.

B. Oil rate

20.

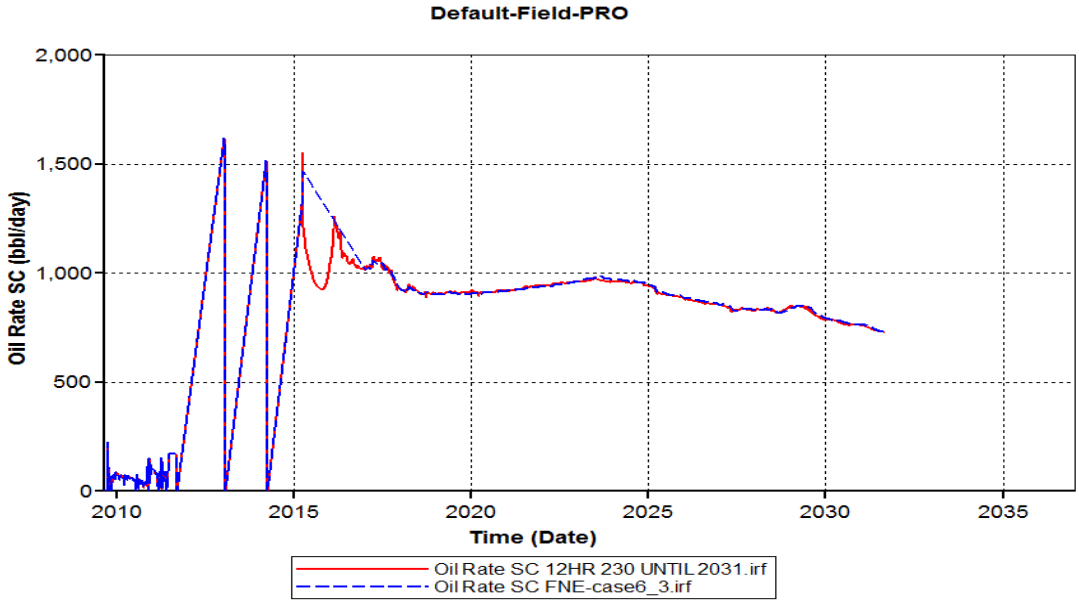

21. Figure (4.22)

C. Overall filed water cut

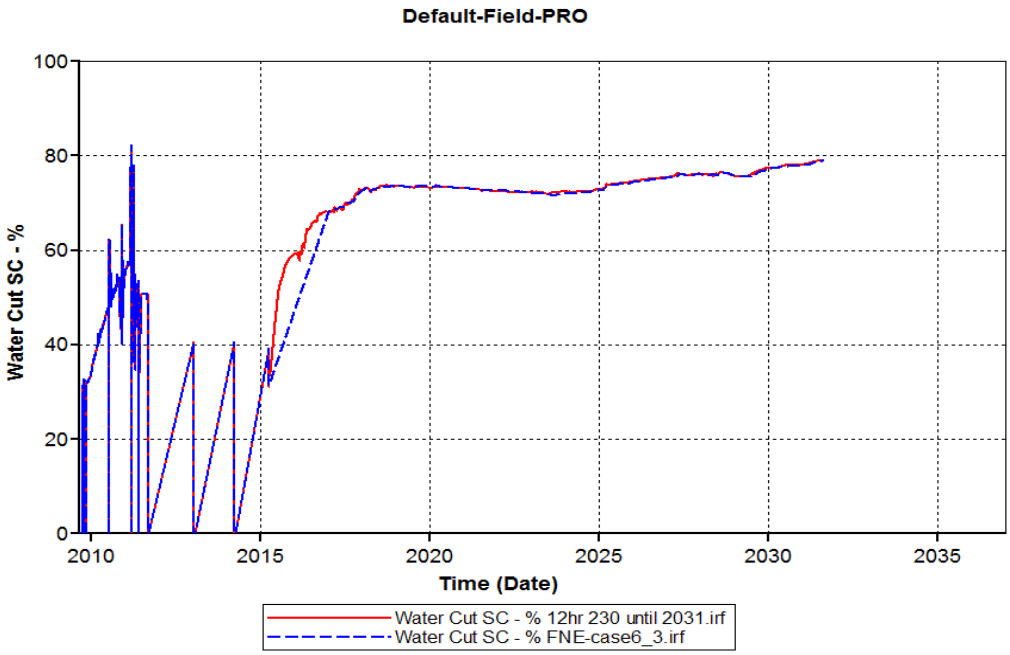

Figure (4.23).22

23. The simulation results also show decreased in oil rate and increased in water cut percent of first scenario at first 21 months (because of incompatibility between the injector condition and reservoir condition) but beyond that the curves MATCH the based case curve.

24.4.2.3.2 The Solar Steam Generation with a Long-term Thermal Storage backup:

25. This scenario discuss the ability of using thermal storage tank to reduce the injection rate for wells that have low fracture pressure or when high injection rate isn't desired, by extending the injection periods for six hour (increasing the injection period to eighteen hour combined).

26. As a result the injection rate required to obtain the same cumulative steam becomes higher than by a factor of 1.33333 (24/18) than the 24 hours continues steam rate (base case)

27. The injection rate required for each well for 18 hours of injection per day (115* 1.33) is 153.33 m^3/day (967.8 bbl/day) as illustrate in the following figure.

(a

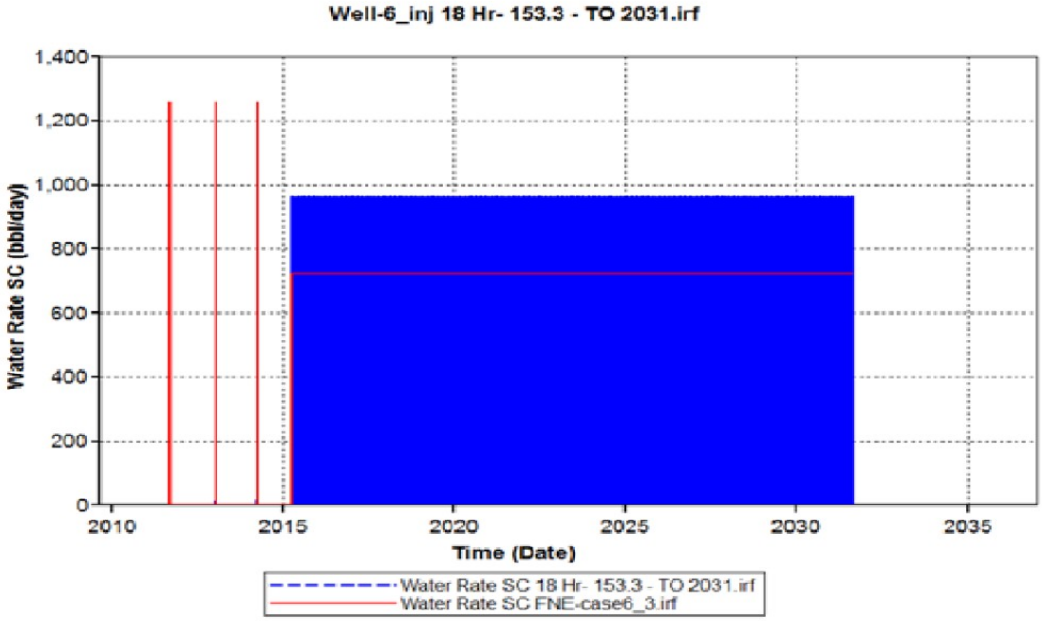

(b (c

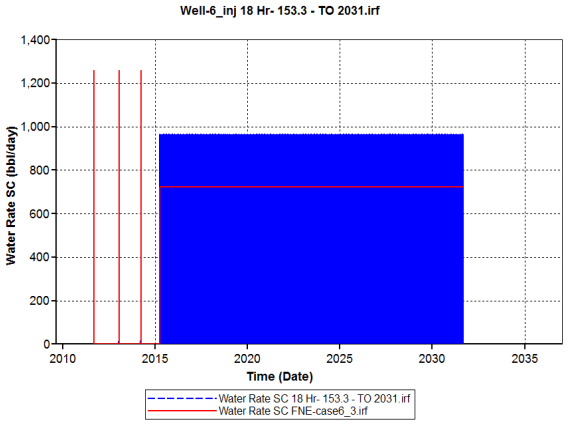

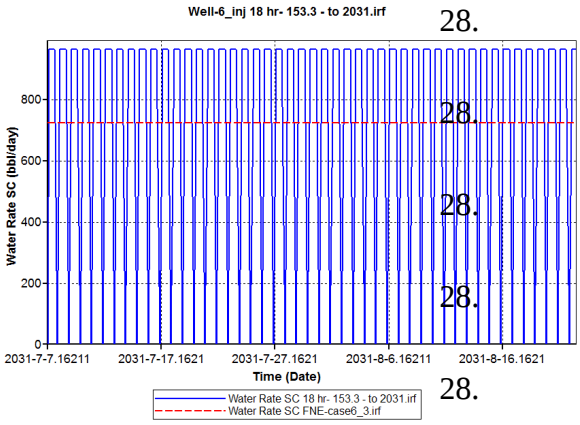

28.

28.

28.

28.

Figure (4.24)

29.

A. cumulative oil production

30.

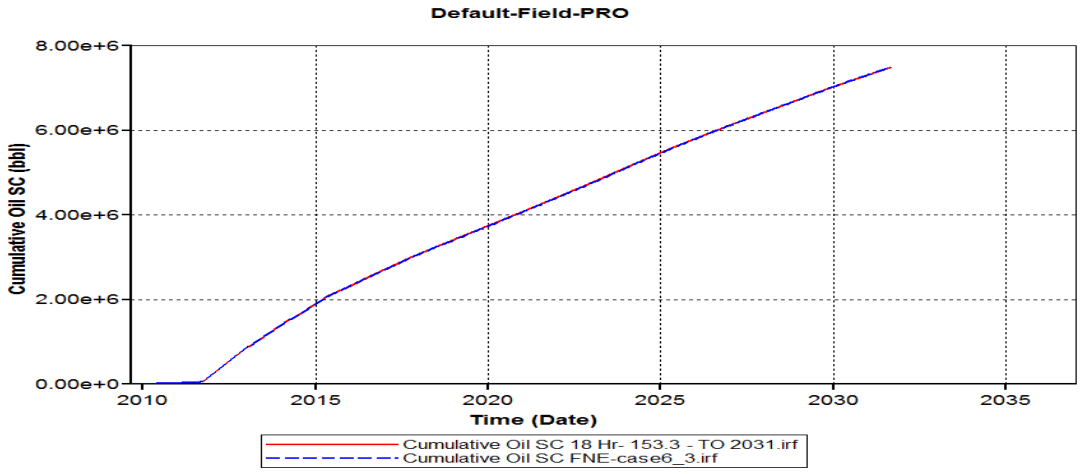

31. Figure (4.25)

B. cumulative water production

.32

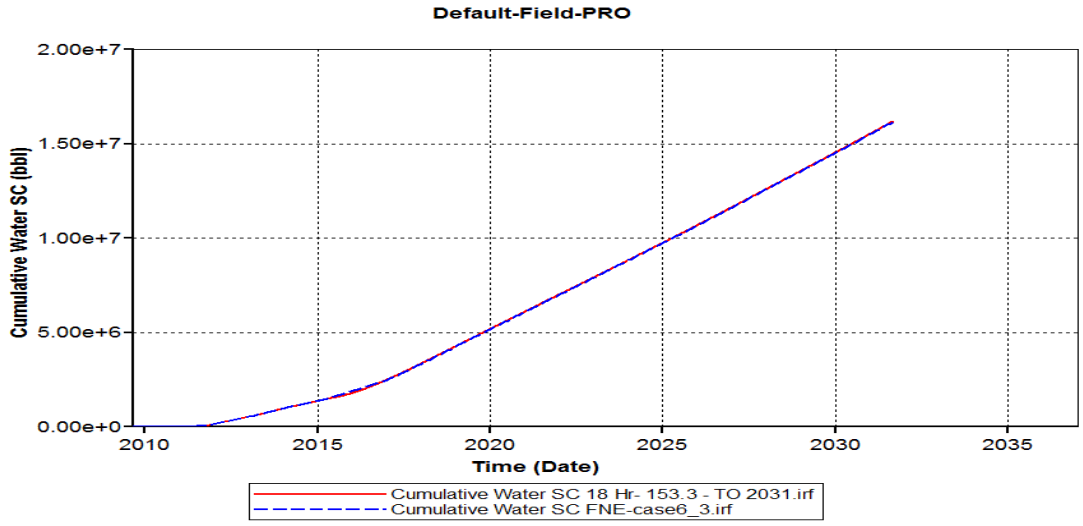

33. Figure (4.26)

34. As in the first scenario simulation results in figure (4.25) and figure (4.26), shows that the cumulative oil production curve and cumulative water

production curve for first scenario MATCH the based case curves, therefore no obvious negative effect observed.

C. Field oil rate:

35.

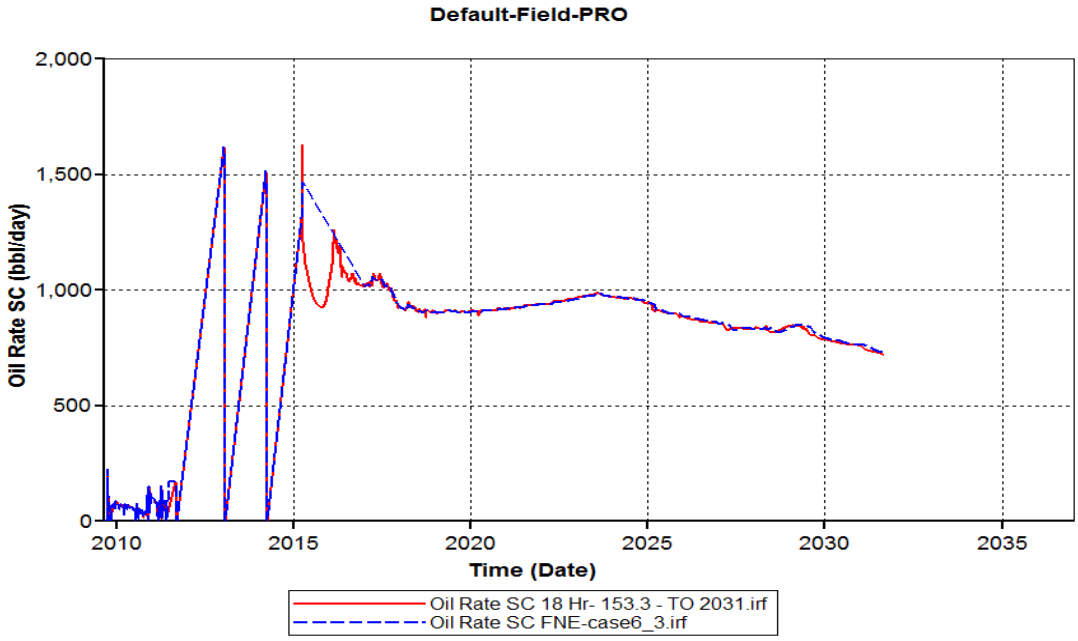

36. Figure (4.27)

37. E. Overall filed water cut

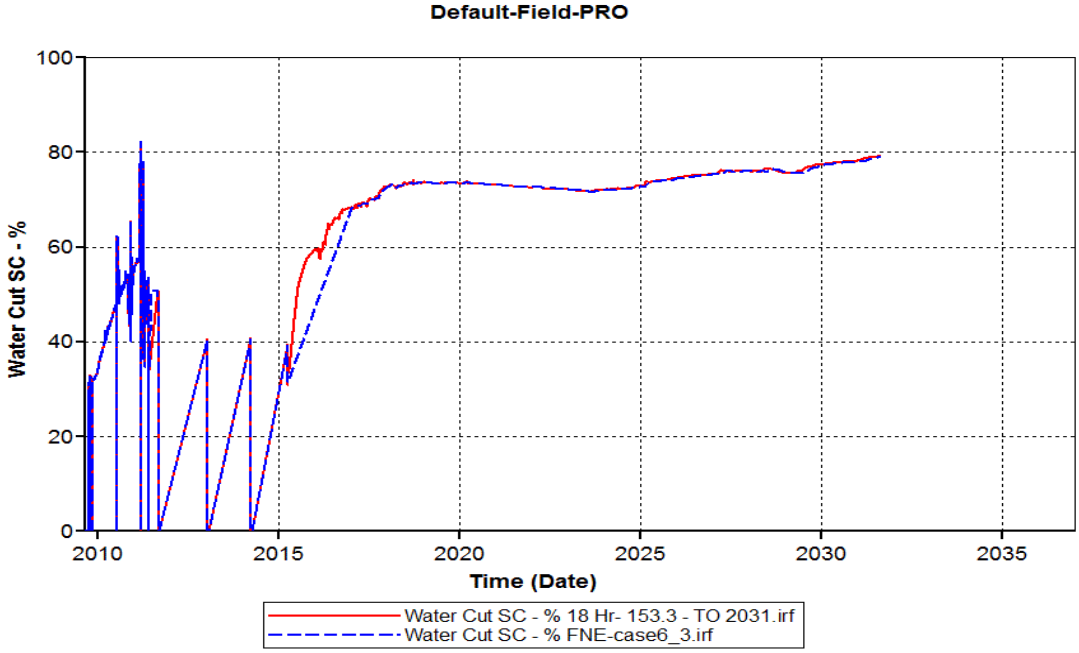

38. Figure (4.28)

39. In term of oil rate and field water cut simulation results also show the same decreased in oil rate and increased in water cut percent at first 21 months but beyond that the curves MATCH the based case curve

40. Table (4.4): Summary for the cumulative values for the first and second secinario

41. Case	42. Cases Parameters		43. Cumulative Production at 2031/9/1						
	45. Continues injection hours per day (hour)	46. Injection rate for each well (m3/day)	47. C	48. C 49. M	50. C	51. Cum steam 52. MMBLL	53. C	54. Oil 55. Recovery 56. Factor	57. Oil 58. Steam Ratio 59. (bbl/bbl)
60. Base cas	61. 24	62. 115	63. 7.	64. 1	65. 2	66. 17.66	67. 2	68. 43.302	69. 2.354944

e									
70. First scenario	71. 12	72. 230	73. 7.	74. 1	75. 2	76. 17.66	77. 2	78. 43.2.488	79. 2.2.3581
80. Second scenario	81. 18	82. 153.3	83. 7.	84. 1	85. 2	86. 17.66	87. 2	88. 43.2104	89. 2.35988

90.

91. As observed in the table (4.4), the result shows that the change in steam injection rate that follows each scenario don't affect the cumulative oil and water production significantly and give very close results.

92.

93. Section three:

94. The Effect of change in Seasons on the Performance

95. As discussed previously, FNE oilfield location shows considerable reduction in solar radiation (among other meteorological parameters) when compared with Amal oilfield location during autumn season (from June to October) as observed in figure (4.30).

96.

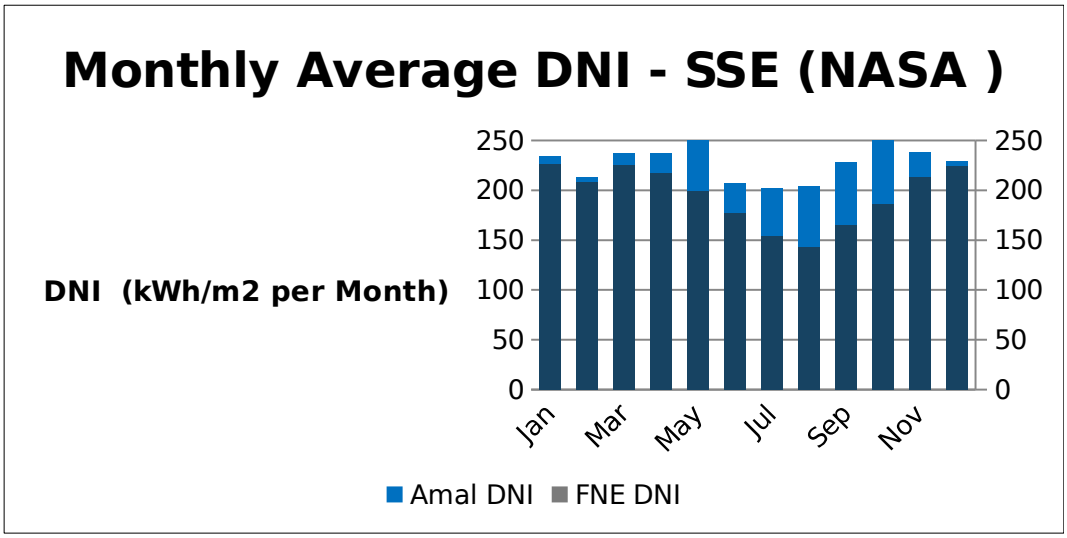

Where all the values blew the average DNI value (192KWH/m^2/month) (which is very close the minimum DNI for Amal field = 201.8 KWH/m^2/month) are consider high and those below the average value are considered Low DNI values.

97. Figure (4.29)

98. Note: SSE NASA data where considered despite its accuracy, because it shows the highest effect of the seasonal variation on the monthly average DNI values at FNE field location.

99. And As Discussed in Chapter 3, two approaches have been proposed in attempt to address the effect of seasonal variation in term of steam injection rate on

the performance of the proposed operation scenarios, where the performance was measured by the same parameters present earlier. And both of them attempt to relate the solar steam rate profile with the Monthly average DNI data at the field location.

100. Discussion for the two approaches is based on comparing the simulation result with the base case and with simulation results for the operation scenarios presented previously.

101. 4.3.1 First Approach:

102. This approach is based on Van Heel et al study, but assumed that the solar generated steam rate will increase by 25% during the months with high solar radiation (January to April, and November and December) and decrease by 25% during the months with low solar radiation (from June to October). As describe by figure (4.30).

103. Note: the DNI values at May (199.33 KWH/m^2/month) are very close to the average DNI value (192KWH/m^2/month), so no change in the injection rate was made.

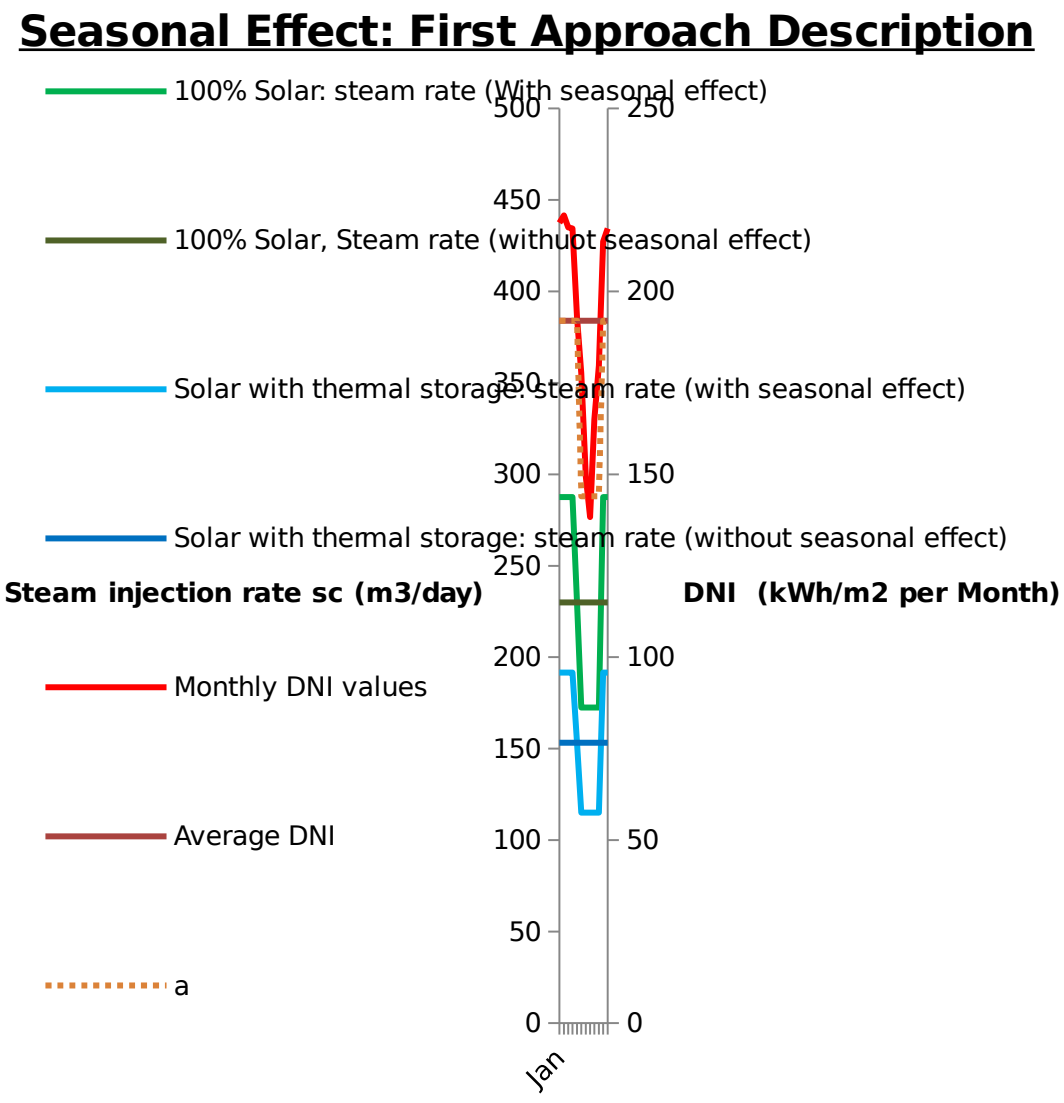
Seasonal Effect: First Approach Description
100% Solar: steam rate (With seasonal effect)
100% Solar, Steam rate (without seasonal effect)
Solar with thermal storage: steam rate (with seasonal effect)
Solar with thermal storage: steam rate (without seasonal effect)
Steam injection rate sc (m3/day)
DNI (kWh/m2 per Month)
Monthly DNI values
Average DNI
a
500
450
400
350
300
250
200
150
100
50
0
250
200
150
100
50
0
Jan

Figure (4.30)

105.

IV.3.1.2 100% Solar Scenario:

106. The steam injection rate:

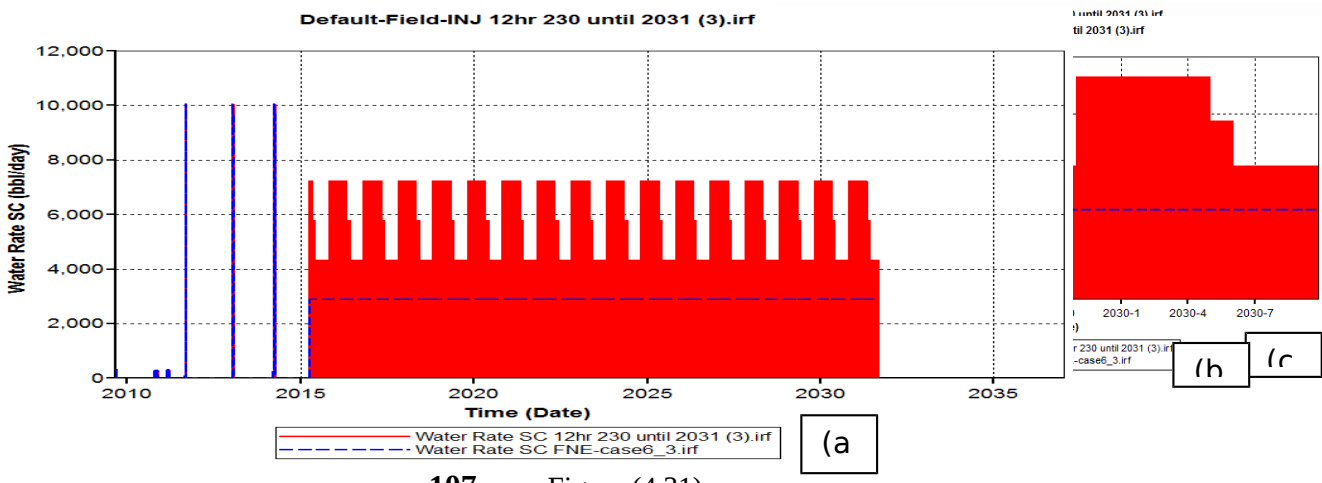

107. Figure (4.31)

108. Figure (4.31): discribe (a) total field injection rate, (b) well 6 injector injection rat as an example. (c) closer view of well 6 injection rate profile for one year.

A. cumulative oil production

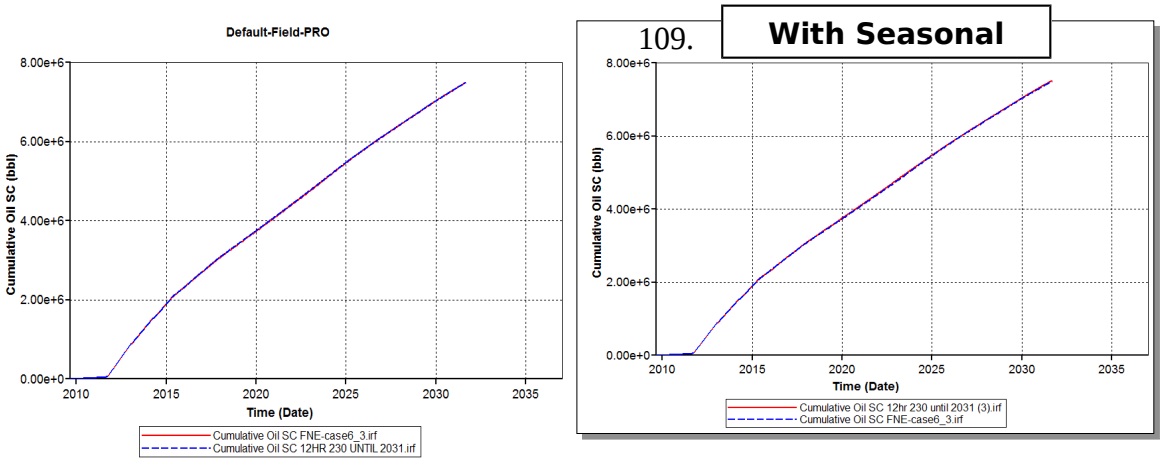

109. Figure (4.32)

B. cumulative water production

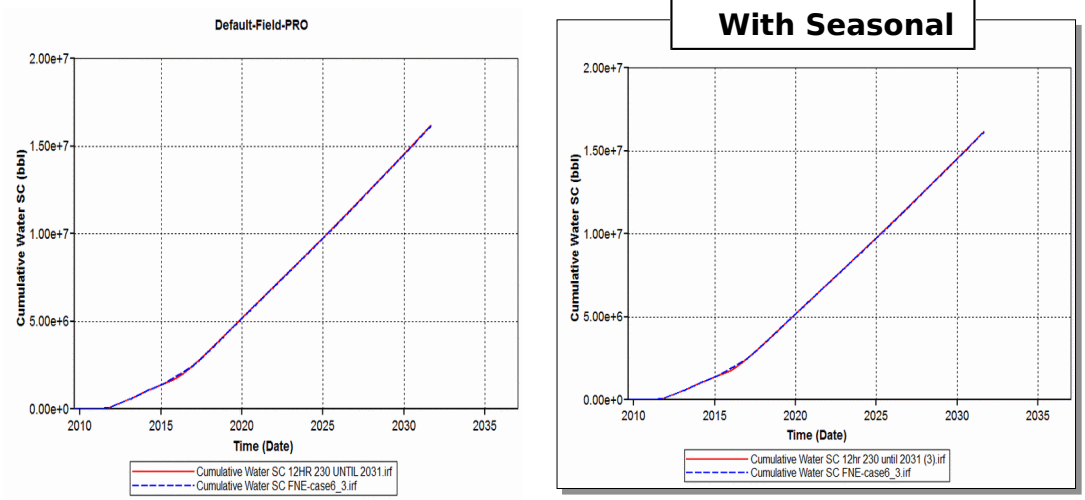

110. Figure (4.33)

111. As in figures (4.32) and (4.33) The simulation results shows that even though the injection rate was occasionally variable through the year the cumulative oil production curve and cumulative water production curve for the first scenario MATCH the based case curves, therefore still no negative effect was observed.

C. Oil rate

112.

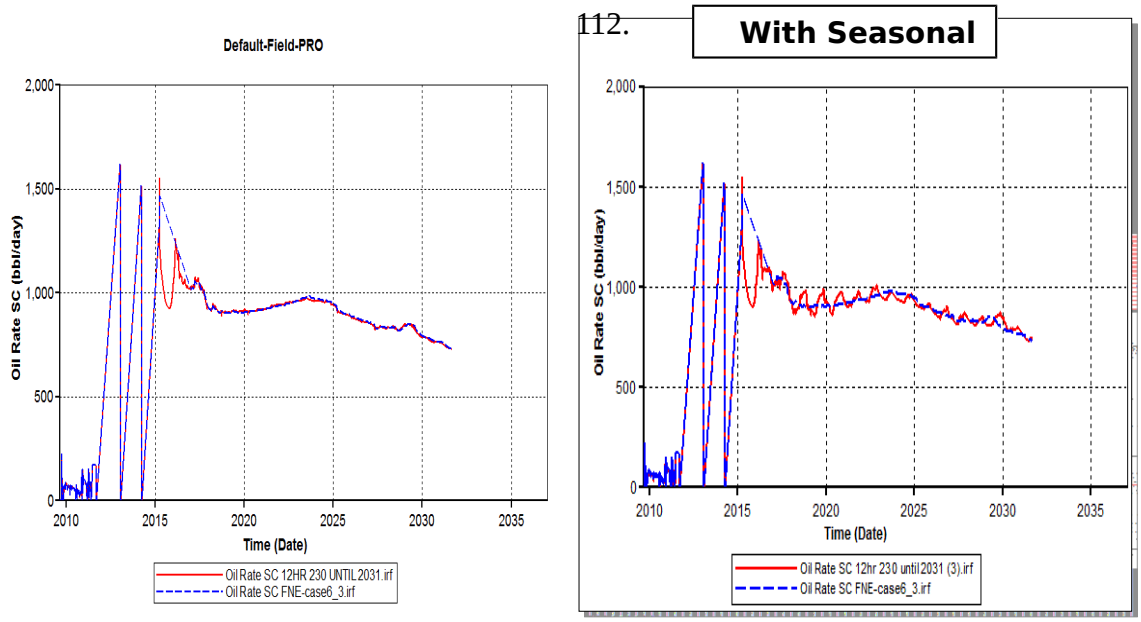

Figure (4.34)

D. Overall filed water cut

Figure (4.35) .

113

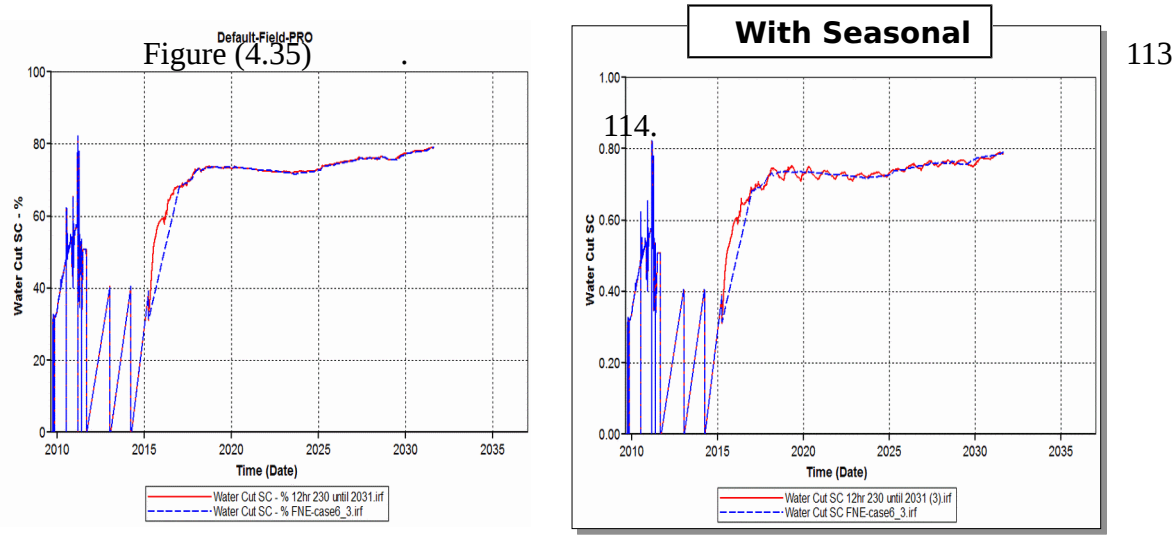

114.

114. The simulation results as expressed in figures (4.34) and (4.35), also shows flocculate on the curves of oil rate and in field water cut following the occasional variation in the injection rate throughout year.

115. 4.3.1.2 The Solar Steam Generation with a Long-term Thermal Storage backup:

116. The steam injection rate:

(b (c

117.

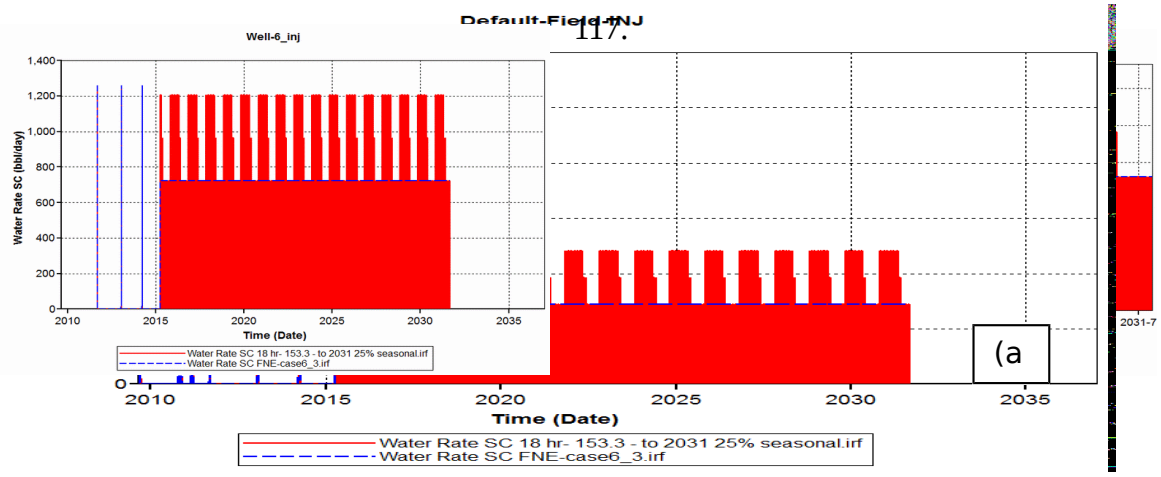

Figure (4.36)

A. cumulative oil production

118.

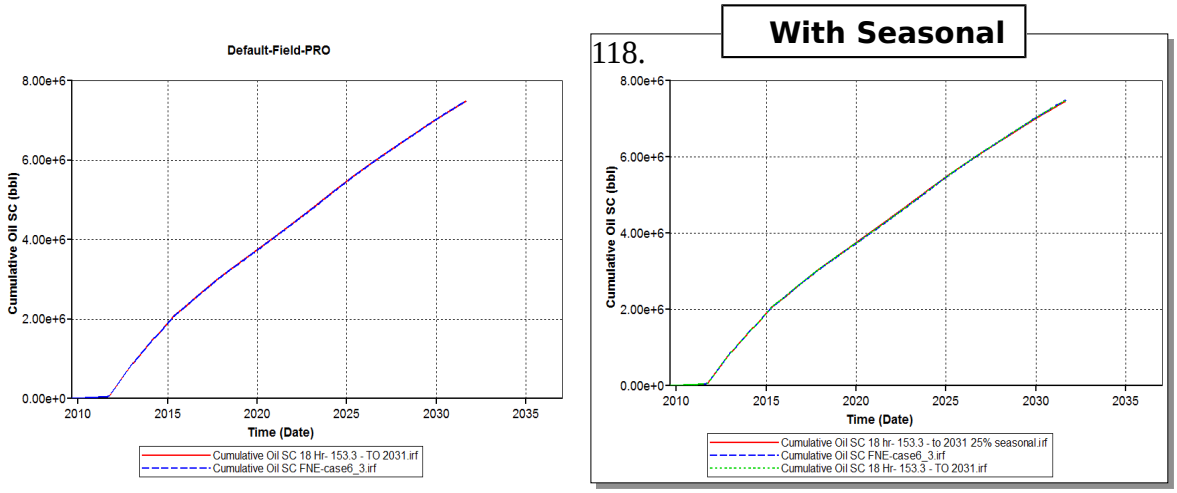

Figure (4.37)

B. cumulative water production

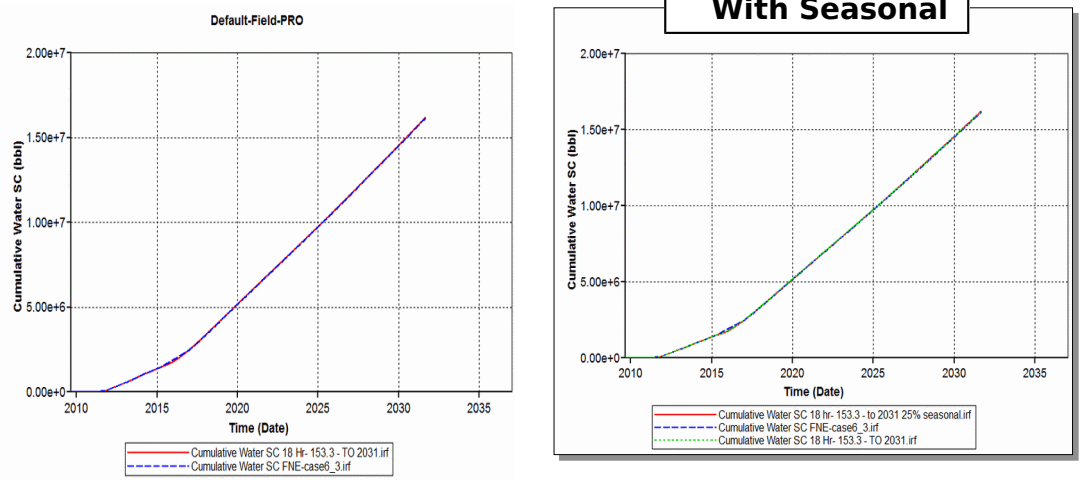

119. Figure (4.38)

120. As in figures (4.37) and (4.38), the simulation results as shows first scenario the cumulative oil production curve and cumulative water production curve for the first scenario MATCH the based case curves, therefore still no negative effect was observed despite the occasional flocculation in injection rate.

121.

C. Oil rate

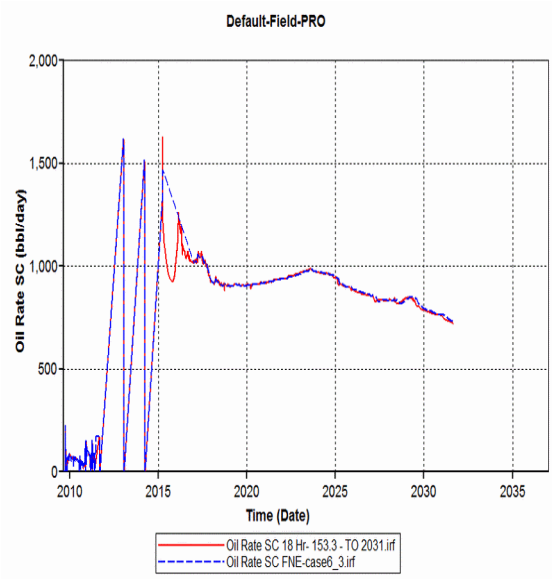

122. Figure (4.39)

D.

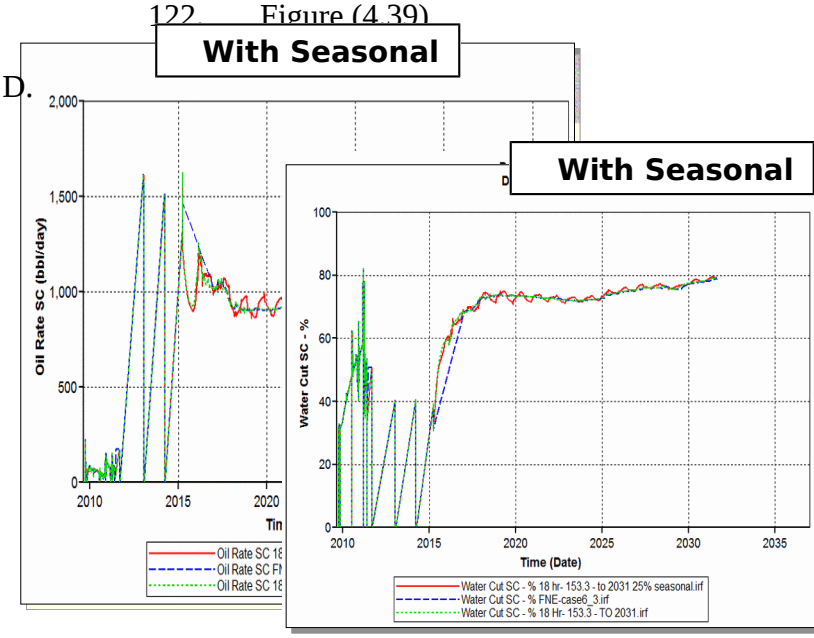

Overall filed water cut

Figure (4.40) .123

124. The simulation results as expressed in figures (4.39) and (4.40), also shows flocculate on the curves of oil rate and in field water cut following the occasional variation in the injection rate throughout year.

125.

126. 4.3.2 Second Approach:

127. This approach based on the performance forecasting of the Solar EOR system deployed in Amal oilfield, and this approach assumed that variation in the DNI values result in an equivalent change in the steam injection rate, i.e. any increase or decrease in the average DNI value result in an equivalent increase or decrease in the steam injection rate. As described in the following figure (figure (4.41)).

128.

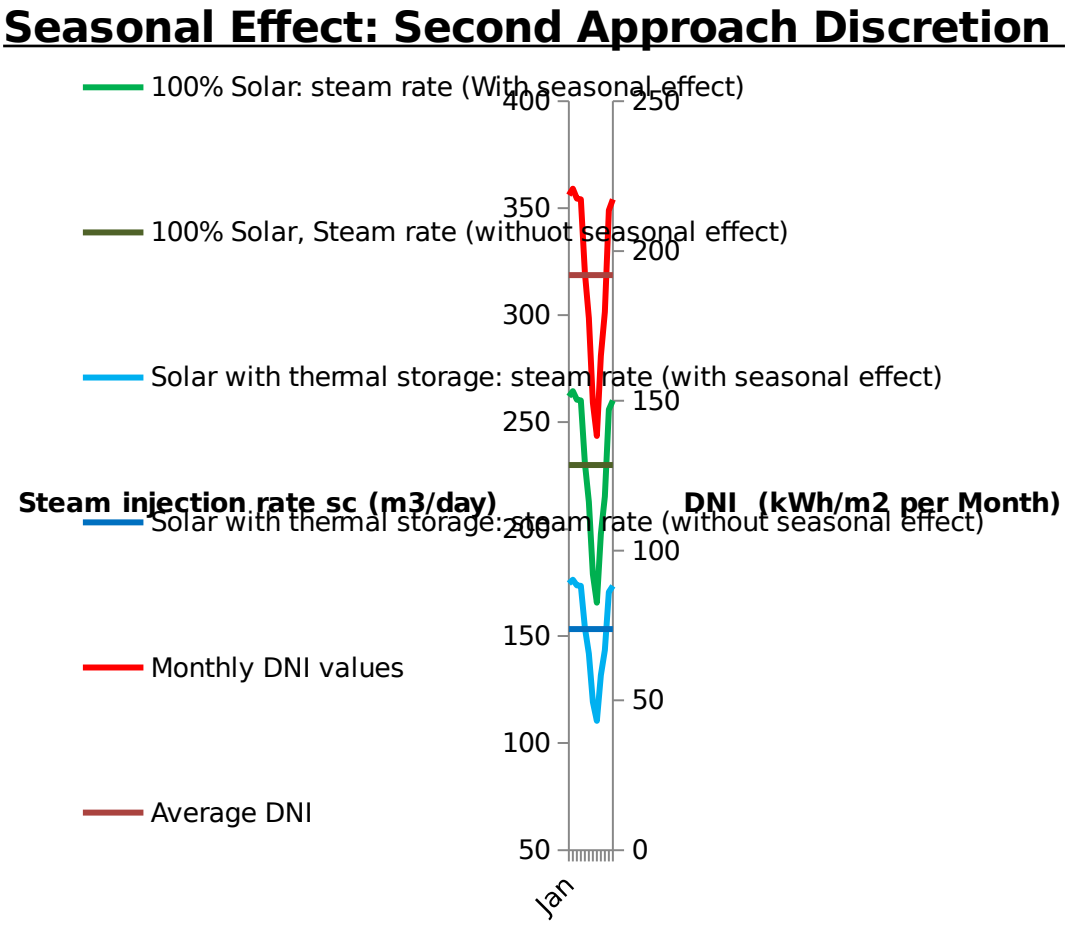

129. Figure (4.41)

130.

131. 4.3.2.1 100% Solar Steam Generation:

132. The steam injection rate:

(a

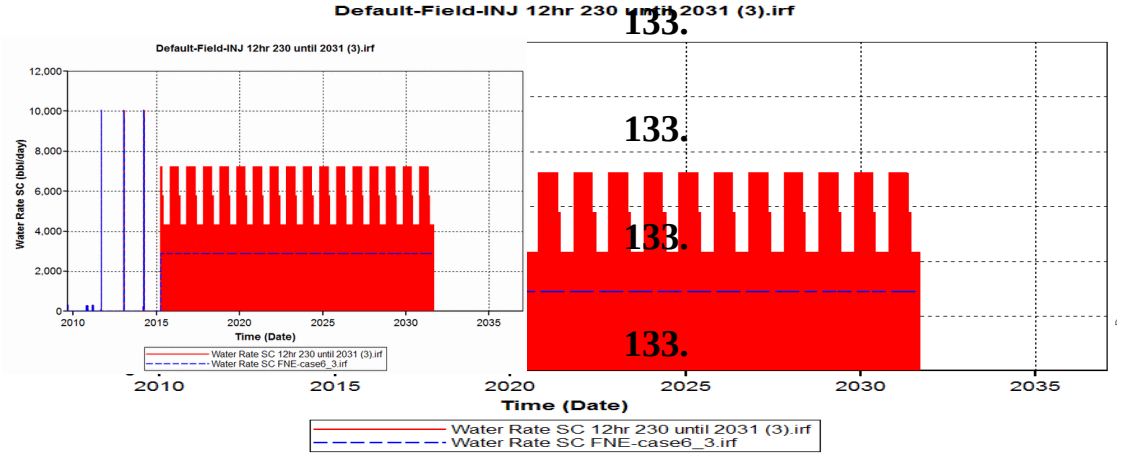

133.

133.

134. Figure (4.42)

A. cumulative oil production

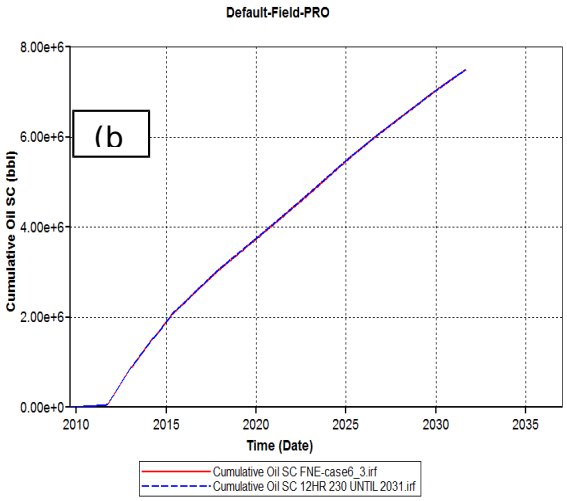

(b

135.

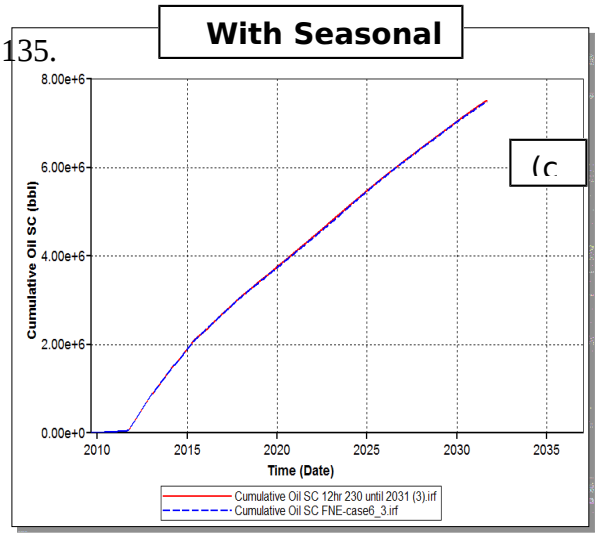

(c

Figure (4.43)

B. cumulative water production

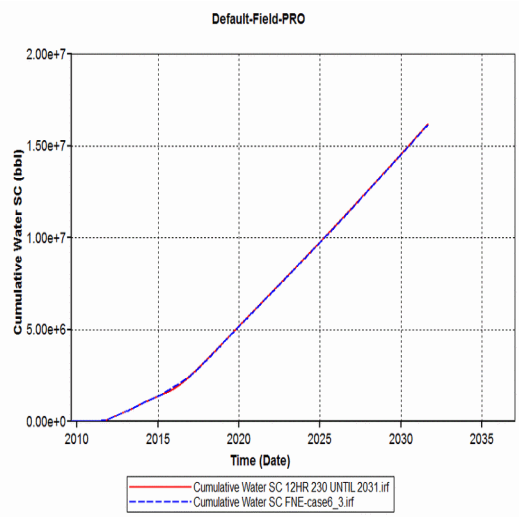

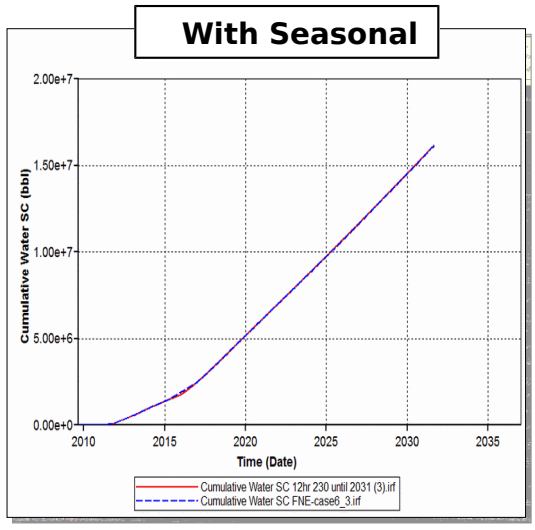

136. Figure (4.44)

137. As in figures (4.43) and (4.44) The simulation results shows that even though the injection rate was monthly variable throughout the year the cumulative oil production curve and cumulative water production curve for the first scenario MATCH the based case curves, therefore still no negative effect was observed also.

C. Oil rate

138.

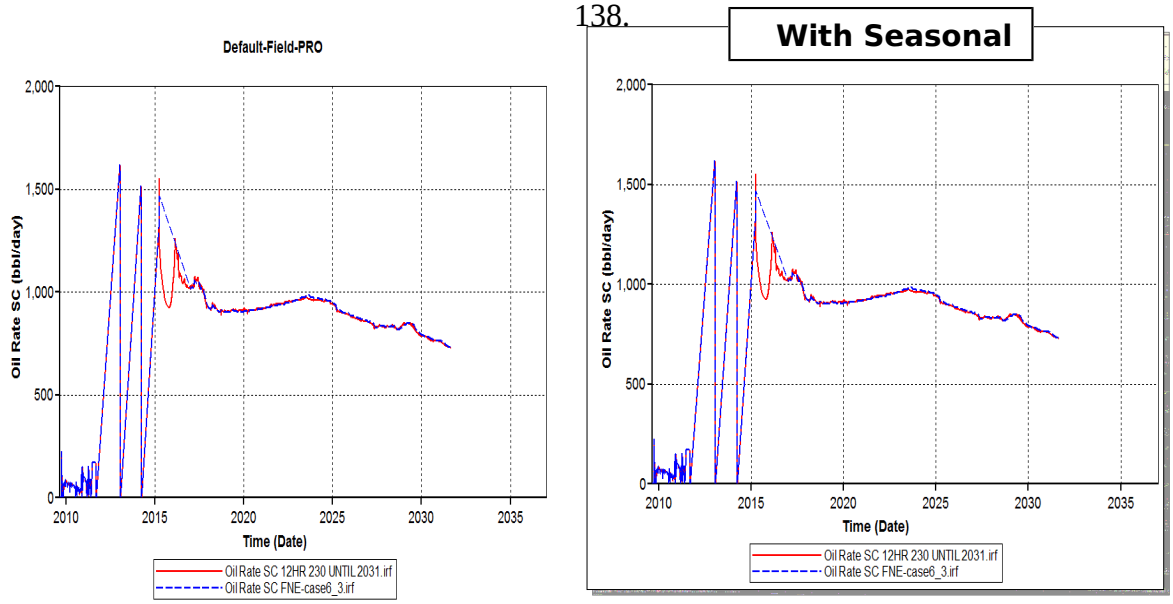

Figure (4.45)

D. Overall filed water cut

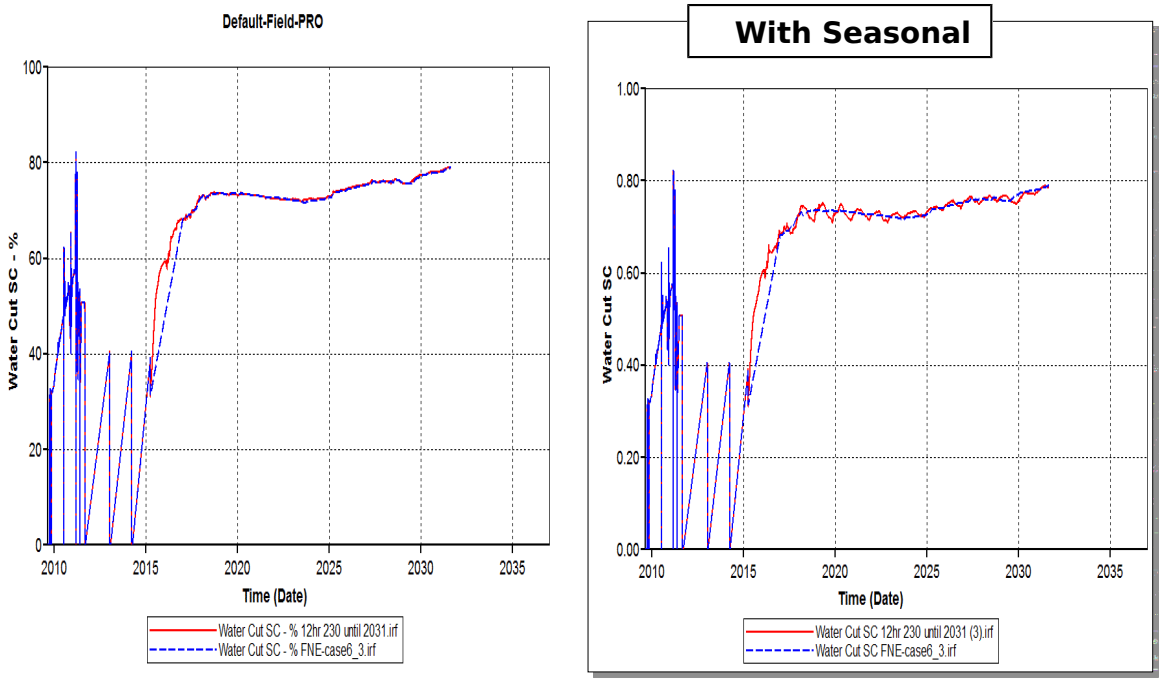

.139 Figure (4.46)

140. The simulation results as expressed in figure (4.46), also shows flocculate on the curves of oil rate and in field water cut following the occasional variation in the injection rate throughout year.

141.

142.

143.

144.

145.

146.

147.

148.

149.

150. 4.3.2.1 The Solar Steam Generation with a Long-term Thermal Storage backup:

151. The steam injection rate:

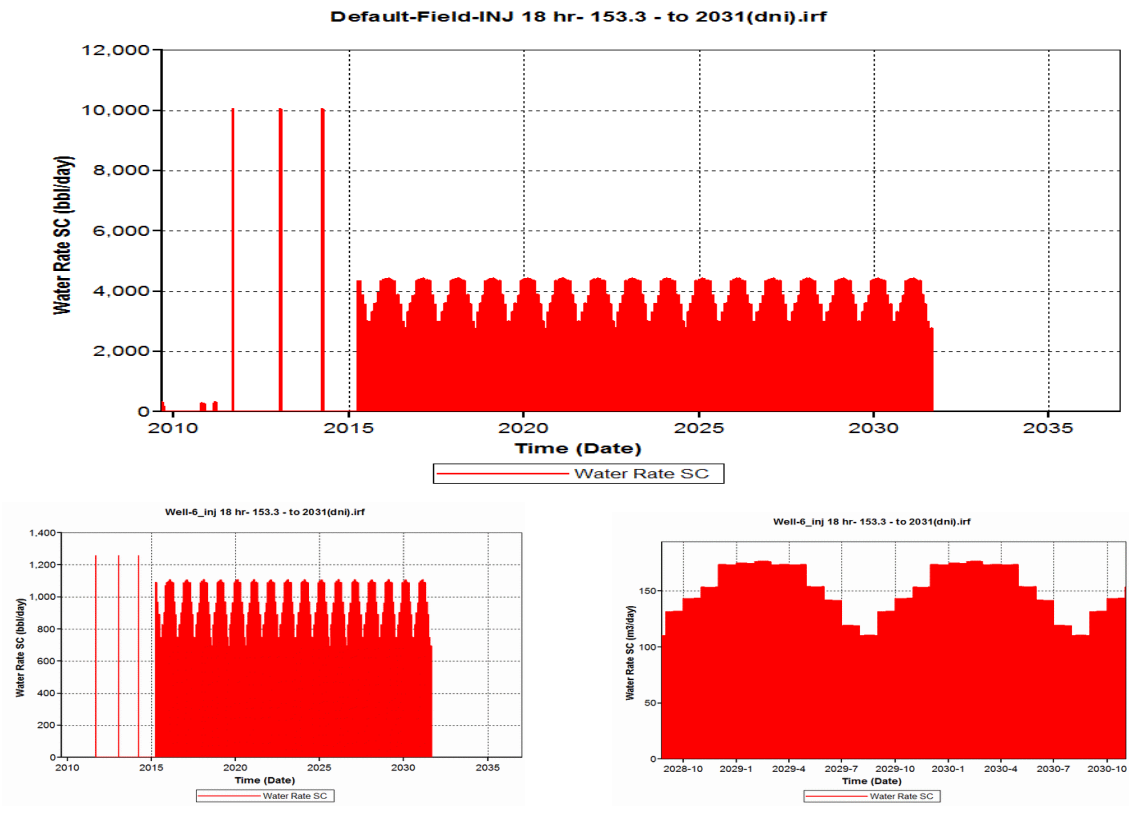

Figure (4.47)

A. cumulative oil production

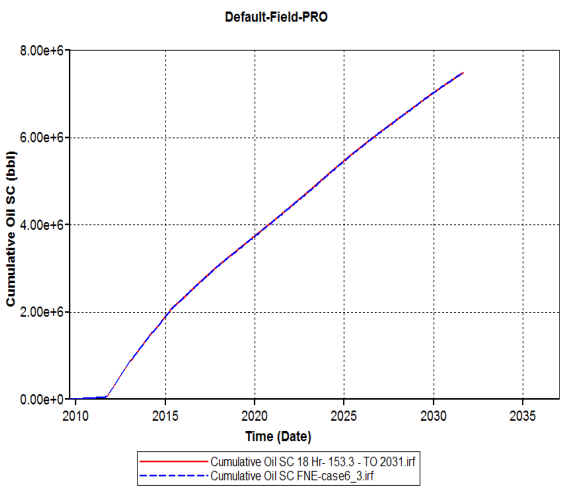

153.

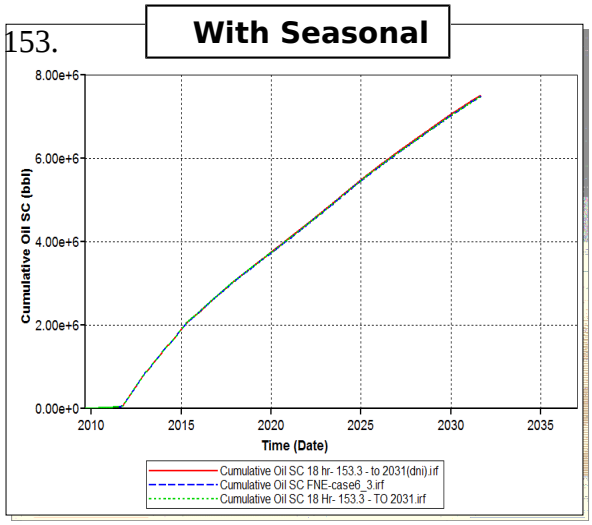

Figure (4.48)

B. cumulative water production

154.

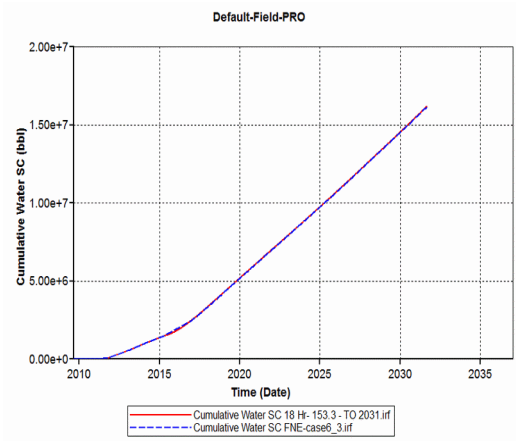

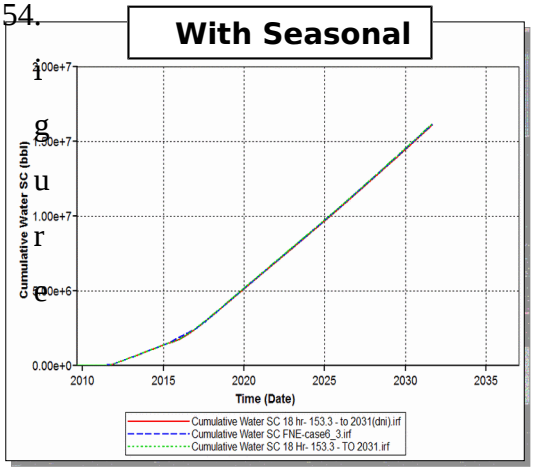

F
i
g
u
r
e

(4.49)

155. As in figures (4.48) and (4.49), the simulation results as shows first scenario the cumulative oil production curve and cumulative water production curve for the first scenario MATCH the based case curves, therefore still no negative effect was observed despite the monthly flocculation in injection rate.

156.

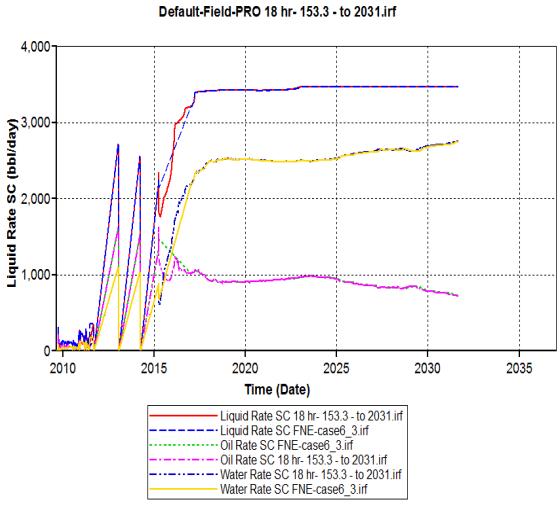

C. Oil rate

157.

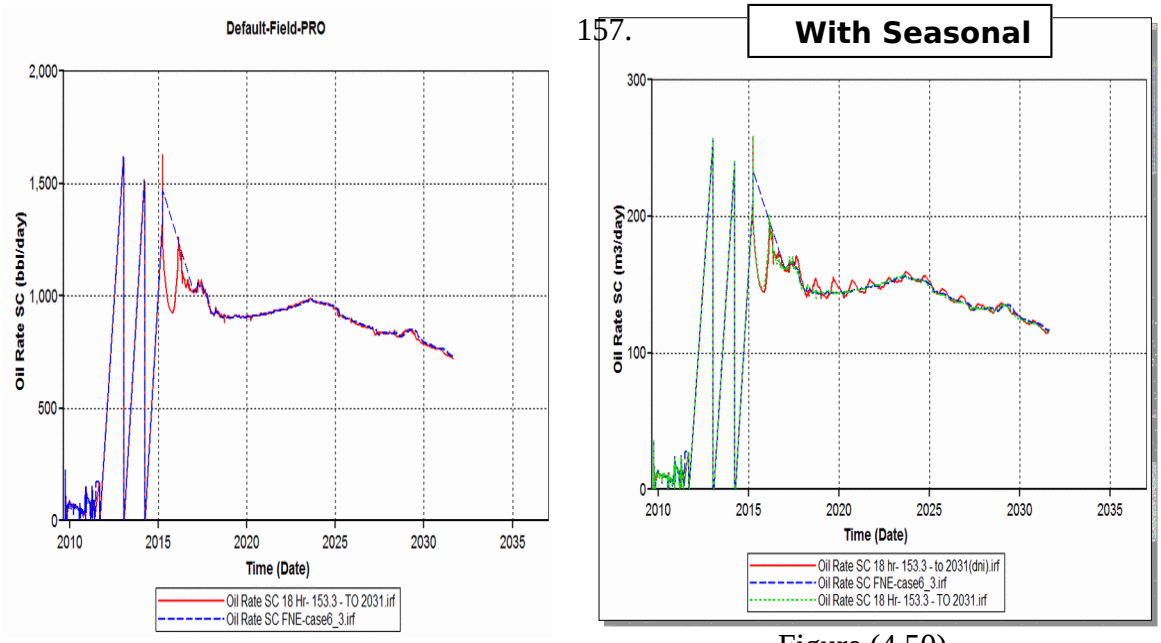

Figure (4.50)

D. Overall filed water cut

Figure (4.51) .158

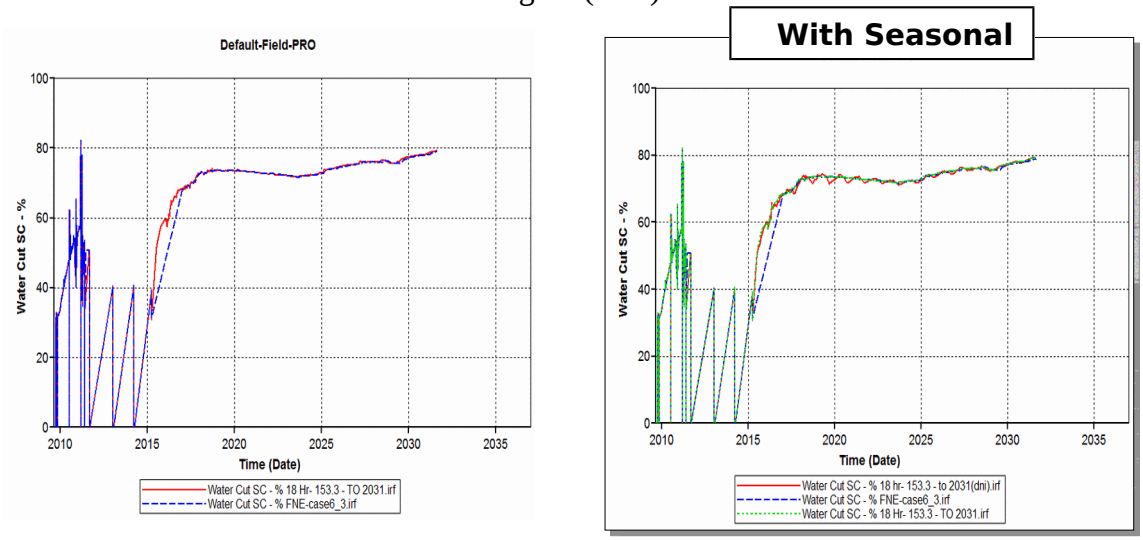

159. The simulation results as expressed in figures (4.50) and (4.51), also shows flocculate on the curves of oil rate and in field water cut following the occasional variation in the injection rate throughout year.

160.

161. Table (4.5):

162.Case		163.Cases Parameters		164.Cumulative Production at 2031/9/1						
		166.Continuesinjectionhoursperday 167.(hour)	168. Inje 169. (m^3/	170. O 171. M	172. Wa 173. M	174. Liq 175. M	176.Steam 177.MMBLL	178. W	179.Oil 180.Recovery 181.Factor	182. Oil 183. Ste 184. (bbl
185.Base case		186.24	187. 115	188.7	189. 16.	190. 23.	191.17.658	192. 2.	193.43.302	194. 2.3
195. First Approach	196. Firs	197. 12	198. 230	199.7	200. 16.	201. 23.	202.17.937	203. 2.	204.43.378	205. 2.3
	207. Sec	208.18	209. 153	210.7	211. 16.	212. 23.	213.17	214. 2.	215.43	216. 2.4

							.938		.083	
217. Second Approach	218. Firs	219.12	220. 230	221. 7	222. 16.	223. 23.	224.17.6267	225. 2.	226.43.37388	227. 2.3
	229. Sec	230.18	231. 153	232. 7	233. 16.	234. 23.	235.17.4692	236. 2.	237.43.38005	238. 2.3

239. As observed in the table (4.5), the result shows that the flocculation in steam injection rate that follows seasonal variation don't affect the cumulative production negatively and in fact increase in cumulative oil recovery was observed in the second approach although no increase in the cumulative steam injection occur.

240.

241.

242. Sensitivity for injection rate:

243. This scenario have been proposed to address the effect of low injectivity on the reservoir hence all the scenarios proposed an increase in injection rate where the cumulative steam injected is the same gives equivalent result have been proved in previous sections here we reduced the injection rate to half in two scenario in base case and in 12hr solar scenario the table (4.6) show simulation result.

244. Table (4.6)

245. Case	246. Casas Parameters		247. Cumulative Production at 2031/9/1					
	251. Continues injection hours per day (hour)	252. Injection rate for each well (m3/day)	253. C	254. C 255. M	256. Cu	257. Cum steam 258. MMBLL	259. C	248. W 249. %
261. Base case (with half the injection rate)	262. 24	263. 57.5	264. 6	265. 9	266. 15.	267. 8.98	268. 1.	269. 6
270. Solar	271. 12	272. 115	273. 6	274. 9	275. 15.	276. 8.95	277. 1.	278. 6

279.

280. No significant change was observed in the cumulative oil and water, the cumulative WOR , oil rate or water rate when comparing the two cases result as illustrate by the figures (a - h) and table (4.6).

281.

282.

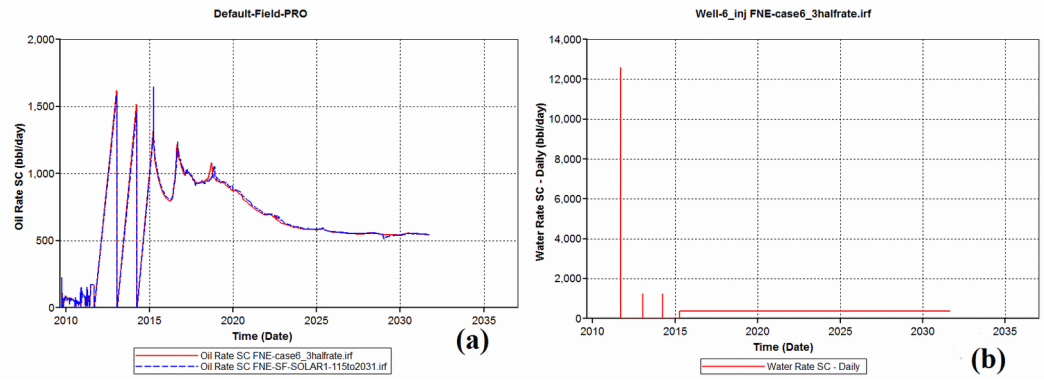
Default-Field-PRO
Oil Rate SC (bbl/day)
2,000
1,500
1,000
500
0
2010
2015
2020
2025
2030
2035
Time (Date)
Oil Rate SC FNE-case6_3halfrate.irf
Oil Rate SC FNE-SF-SOLAR1-115to2031.irf
(a)
Well-6_inj FNE-case6_3halfrate.irf
Water Rate SC - Daily (bbl/day)
14,000
12,000
10,000
8,000
6,000
4,000
2,000
0
2010
2015
2020
2025
2030
2035
Time (Date)
Water Rate SC - Daily
(b)

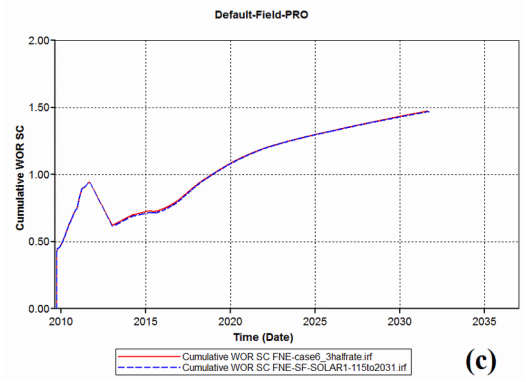
Default-Field-PRO
Cumulative WOR SC
2.00
1.50
1.00
0.50
0.00
2010
2015
2020
2025
2030
2035
Time (Date)
Cumulative WOR SC FNE-case6_3halfrate.irf
Cumulative WOR SC FNE-SF-SOLAR1-115to2031.irf
(c)

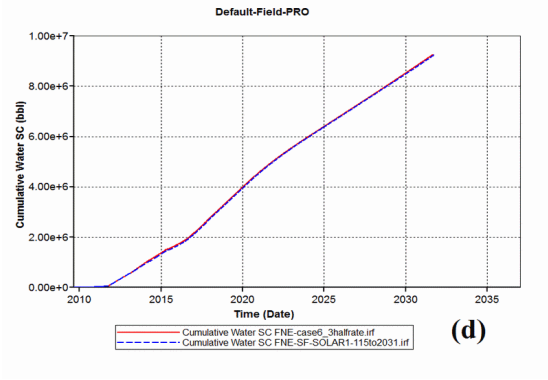
Default-Field-PRO
Cumulative Water SC (bbl)
1.00e+7
8.00e+6
6.00e+6
4.00e+6
2.00e+6
0.00e+0
2010
2015
2020
2025
2030
2035
Time (Date)
Cumulative Water SC FNE-case6_3halfrate.irf
Cumulative Water SC FNE-SF-SOLAR1-115to2031.irf
(d)

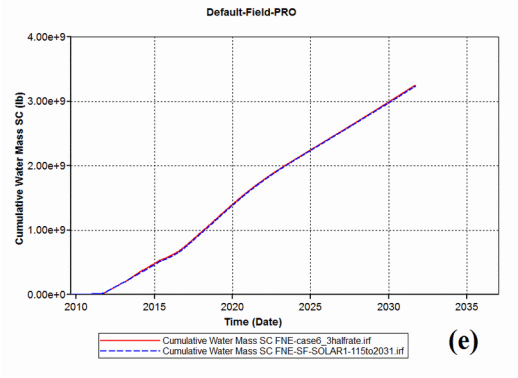
Default-Field-PRO
Cumulative Water Mass SC (lb)
4.00e+9
3.00e+9
2.00e+9
1.00e+9
0.00e+0
2010
2015
2020
2025
2030
2035
Time (Date)
Cumulative Water Mass SC FNE-case6_3halfrate.irf
Cumulative Water Mass SC FNE-SF-SOLAR1-115to2031.irf
(e)

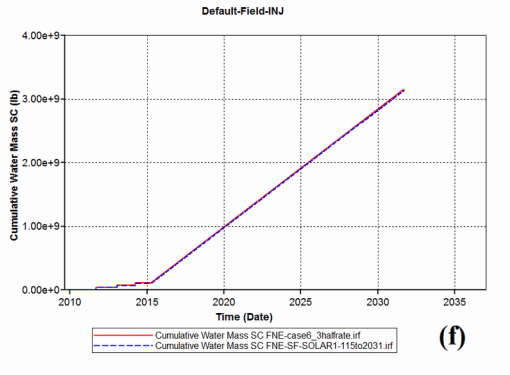

(f)

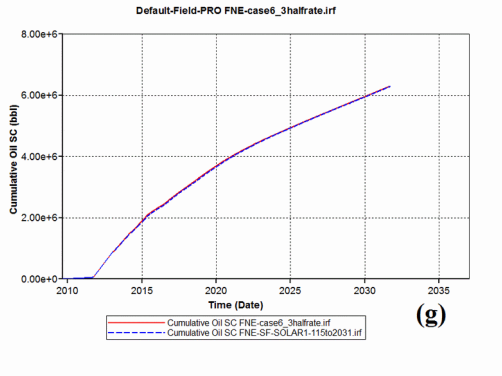

(g)

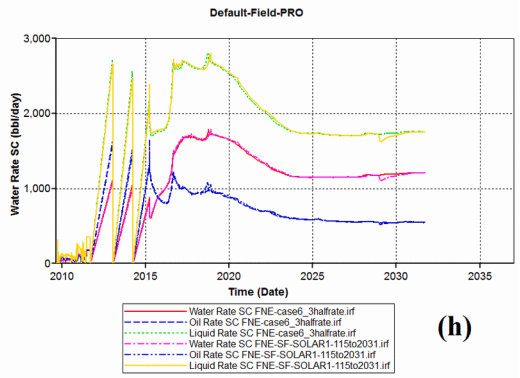

(h)

283.Figure (4.52)

284.

285.

286. Section four:

287. Highlights on the Economic and Environmental Impact

288. 4.

4.1. Fuel gas consumption:

289. Th

e amount of gas fuel consumed by the steam generation unit as given from (CPF) report as summarized in table (4.8) represent amount of gas savings associated with implementing

290. Ta

ble (4.8)

291. **Fuel Type**	**292. Daily**	**293. Annual Sum**	**294. ACCUM**
295. Inlet gas to SGU(KM3)	296. 13.71	297. 7 43.3	298. 3112.3
299. Inlet gas to SGU(Mscf)	300. 483.7923379	301. 7 314.07	302. 109825.4481

303.

304. 4.

4.1. Cost of Fuel:

305. The cost associated with natural gas consumption was summarized in table (4.8), where cost of natural gas was calculated at today – 2016/10/12 – natural gas price of (3.22$/scf).

306. Table (4.9)

307. **Cost of Fuel**	**308. Daily 309. ($/day)**	**310. Annual Sum 311. ($/Year)**	**312. ACCUM 313. ($)**
314. First Scenario 315. (%100 Solar Steam generation)	316. 1557811.328	317. 23551305.4	318. 353,637,942.9
319. Second Scenario 320. (Solar Steam generation with Thermal Storage backup)	321. 1557811.328	322. 23551305.4	323. 353637942.9

324. Third Scenario 325. (Solar Steam generation with natural gas backup)	326. 778905.664	327. 11775652.7	328. 176818971.4

329.

330. As the table illustrate, the total cost savings associated with natural gas consumption when implementing the 100% solar scenario and solar steam generation with thermal storage backup reach up to 353.64 Million dollars in total, with a constant daily operation cost of 1.56 Million dollars per day after fifteen years.

331. 4.4.2. Environmental impact:

332. Using solar energy as a replacement of natural gas for thermal EOR can thus lead to a reduction in emissions of CO2, NOx and CH_4 . Table(4.7) estimation factors for different greenhouse gases (GHG) emission at different units as published by Intergovernmental Panel on Climate Change (IPCC).

333. Table (4.10):

334.	335. Heatin	337. CO_2	340. CH_4	343. N_2O	346. CO	349. CH	352. N
1. **Fuel Type**		2. CO_2 3. **Metric tone**		4. **Kg** CH_4 per mmBtu		5. **Kg** N_2O per mmBtu	**353. Fa** 354. g
6. Daily		7. 26.33765488		8. 0.498306		9. 0.048379	
10. Annually		11. 398.1779708		12. 3644.646		13. 353.8491	
14. Accumulate		15. 5978.897395		16. 4E+08		17. 38861636	
355. Natural Gas (per scf)	356. 0.001026	357. 53.06	358. 1	359. 0.1	360. 0.0	361. 0.0	362. 0.

363.

364. Table (4.7): GHG factors published by Intergovernmental Panel on Climate Change (IPCC), Fourth Assessment Report (AR4), 2007

365. Table (4.11):

366.

367. As table (4.9) show almost four huondrd tones of GHGs are emitted annually and the pilot has emitted about six thousand tons of GHGs so far and continue to do so, these amounts of emission are equivalent of emission of 676,188 gallons of burnt gasoline. (as calculated by the US Environmental Protection Agency EPA)